BRITISH ECOLOGICAL SOCIETY Functional Ecology

When is the bait worth the risk? A mechanistic model of a compensatory ecological trap in seabirds

Journal:	*Functional Ecology*
Manuscript ID	FE-2025-01675
Wiley - Manuscript type:	Research Article
Key-words:	trophic subsidy, bycatch, life-history, fisheries

Abstract

Ecological traps—preference–performance mismatches that reduce fitness—are expected in vertebrate–fishery systems worldwide, yet this mechanism has seldom been made explicit in explaining declines driven by subsidy–bycatch interactions. Here, focusing on seabirds, we develop and test a mechanistic hypothesis for a compensatory trap in which fishery-derived trophic subsidies (bait, catches, and especially discards) increase foraging success and thus habitat preference around vessels, which can boost breeder and fledgling recruitment while reducing lifetime reproductive success through bycatch—a trap mechanism likely common and readily generalizable across marine vertebrates, including mammals, turtles, and elasmobranchs. Specifically, we develop a spatially explicit, individual-based model spanning slow, intermediate, and fast life-history strategies to evaluate when and how traps emerge. The model predicts nonlinear, threshold responses governed by life-history strategy: when bycatch is low, subsidies yield net population gains; beyond species-specific bycatch thresholds, the same subsidies reinforce maladaptive selection and accelerate declines. In some regimes, short-term recruitment gains can yield transient increases while masking long-term fitness costs and subsequent population decline, hindering trap detection and management. Consistent with life-history theory and empirical evidence, slow-lived species (albatrosses) face the greatest risk of falling into a trap under equivalent subsidy–bycatch regimes. Our results extend ecological-trap theory by embedding explicit vital-rate trade-offs and clarifying how trophic subsidies and bycatch interact along the slow–fast life-history continuum to determine when traps emerge and how they filter species by strategy. Crucially, we argue for integrated management of bycatch and discards, whose interdependent effects can reinforce maladaptive habitat selection and elevate extinction risk. Framed mechanistically, system-specific compensatory-trap models can provide actionable predictions and thresholds for conservation and management strategies.

Keywords: trophic subsidy, discards, bycatch, life-history, fisheries

1. Introduction

A common assumption in ecology is that an organism's ability to survive and reproduce is closely linked to its habitat preferences, which have been shaped by natural selection. However, organisms do not always make adaptive choices and may find a habitat equally or more attractive than other available options, despite experiencing reduced fitness having selected it—a phenomenon known as ecological traps (Dwernychuk and Boag, 1972; Gates and Gysel, 1978). Theory shows that traps heighten the risk of extinction for local populations and spatially structured metapopulations (Delibes et al., 2001; Donovan and Thompson, 2001; Fletcher et al., 2012; Hale et al., 2015; Kokko and Sutherland, 2001; Kristan et al., 2003). Empirical evidence further indicates that ecological traps are widespread in terrestrial and marine ecosystems and frequently result from rapid, human-driven environmental change that outpaces adaptive responses (Hale and Swearer, 2016; Robertson et al., 2013; Swearer et al., 2021). As these changes persist, ecological traps are likely to become more frequent.

Previous theoretical models typically assume maladaptive habitat selection with respect to either survival or reproduction (Delibes et al., 2001; Donovan and Thompson, 2001; Fletcher et al., 2012; Hale et al., 2015; Kokko and Sutherland, 2001; Kristan et al., 2003). Yet traps may also involve fitness trade-offs, whereby apparently maladaptive behavior in one component (e.g., survival) is offset by gains in another (e.g., reproduction) (Battin 2004). Ecological and evolutionary responses to such trade-offs are expected to depend on life-history strategy, particularly position along the slow–fast continuum (Saether, 1987; Stearns, 1992). Species with a slower pace of life—longer lifespans, lower reproductive potential, and reduced maximum population growth—are predicted to be especially vulnerable to traps (Kokko and Sutherland 2001, Hale et al. 2015b). Introducing trade-off traps can therefore yield outcomes that differ from classical models, within and among species, potentially generating nonlinear population dynamics across the slow–fast continuum with consequences for long-term viability. Understanding the specific mechanisms through which traps influence life histories is thus critical for anticipating, preventing, and managing their demographic effects (Robertson and Blumstein, 2019; Swearer et al., 2021).

A key driver of such compensatory traps may be human-derived trophic subsidies, which provide abundant and predictable food that can enhance foraging success and, in some cases, reproduction(Oro et al. 2013). However, increased habitat preference can also elevate mortality via pollutants, predators, competition, parasitism, hunting, or accidental deaths (Becker et al., 2015; Lamb et al., 2017; Lewison

et al., 2014; Morris, 2005; Rodewald et al., 2011; Semeniuk and Rothley, 2008; Sigaud et al., 2017; Simon and Fortin, 2020). We therefore define compensatory ecological traps as traps in which organisms preferentially select a habitat because one or more fitness components increase (e.g., foraging success and/or reproduction), even as another key component (e.g., survival) is simultaneously reduced. This trade-off can initially mask negative demographic outcomes, particularly when short-term reproductive gains create the illusion of population-level benefits despite reduced lifetime reproductive success and long-term viability.

Seabird–fishery interactions offer a salient example. Trophic subsidies from fishing vessels—bait, offal, and discards—attract seabirds and can enhance foraging success (Oro et al., 2013). At the same time, attraction increases bycatch risk through hooking (e.g., longline; Anderson et al. 2011), entanglement (e.g., purse seine, gillnets; Žydelis et al. 2013, Simeone et al. 2020), or collisions with gear (e.g., trawl; Phillips et al. 2024). Bycatch is a primary at-sea threat to seabirds, contributing to population declines and elevated extinction risk (Dias et al., 2019; Richards et al., 2024, 2021). Conversely, fishery-derived food—specially discards (Bicknell et al., 2013; Garthe et al., 1996; Sherley et al., 2019; Votier et al., 2004)— can increase breeder and fledgling recruitment, potentially offsetting some costs of bycatch mortality (Barbraud et al., 2008; Genovart et al., 2016; Pardo et al., 2017; Rolland et al., 2010, 2008). Such demographic compensation is expected to be stronger in fast-lived species, which are more sensitive to reproduction, than in slow-lived species, which are more sensitive to survival (Heppell et al., 2000; Saether and Bakke, 2000). However, how these compensatory responses are shaped by life-history traits remains unclear (Genovart et al., 2017).

There is strong evidence that fishery-derived subsidies elevate bycatch risk (ACAP, 2024; Favero et al., 2011; González-Zevallos and Yorio, 2006; Sullivan et al., 2006; Watkins et al., 2008). Yet, beyond the 'junk-food' hypothesis where low-quality subsidies reduce reproductive success (Grémillet et al., 2008), the ecological-trap has rarely been used to frame or predict seabird–fishery interactions nor has it been widely extended to other large marine vertebrates (including sea turtles, marine mammals, and elasmobranchs; Lewison et al., 2014). Consequently, we still lack a mechanistic framework—and formal trap models—to understand when subsidy-driven preference and bycatch interact with life-history strategies to give rise to compensatory traps. To address these gaps, we developed a spatially explicit, individual-based model (IBM; Grimm and Railsback, 2005) to evaluate how species with contrasting life histories (slow, intermediate, and fast) respond to a compensatory ecological trap in which individuals

preferentially select areas with enhanced foraging success due to fishery subsidies. This behavior can increase breeder and fledgling recruitment but also elevates bycatch mortality, generating strategy-dependent demographic trade-offs. By integrating ecological-trap theory with life-history theory, our study shows how these trade-offs can produce nonlinear, dynamic population responses, thereby extending the classical trap framework and providing actionable insights for conservation and fisheries management.

2. Methods

2.1. The model

The description of the model follows the protocol created by Grimm et al., (2006) to explain IBM within an ecological framework. Following the description of the model, we explain the experiments conducted in detail. The model was developed in R (R Core Team, 2021) using the NetLogoR (Bauduin et al., 2019), dplyr (Wickham et al., 2023), and data.table (Barrett et al., 2024) packages.

2.2. Model Purpose

The model aims to simulate population responses of species with varying life-history strategies along the slow-fast continuum under compensatory ecological trap scenarios. In our simulation, the compensatory trap is established by introducing additional energy to a limited area of the habitat while simultaneously increasing mortality risk within the same region. This enhanced habitat increases foraging success by allowing individuals to remain longer in high-energy cells, increasing their chances of consuming energy over successive time steps before moving. This reduces the frequency of movement and the energetic costs of search. As a result, it can increase both breeder recruitment (i.e., the proportion of potential breeders that actually reproduce) and the reproductive success of breeders (i.e., the number of chicks fledged per breeding individual). The level of mortality risk is determined by specific trap parameters. The base model is a spatially explicit simulation of the life cycle of a colonial bird. It integrates life-history traits, memory-based foraging behaviors, reproduction, and mortality in a patchy, energy-limited environment that changes dynamically as energy is depleted through foraging activity.

2.3. Entities, state variables, and scales

The model consists of four entities: (1) the population and its associated attributes, (2) an energy raster representing the environment and its attributes, (3) the colony, and (4) the trap raster and its associated attributes (Figure 1). Each individual in the population is defined by five key state variables: identity code, spatial coordinates (both current and from the previous step), age, breeding state, and energy. The identity code is a unique identifier assigned to each individual at the start of the simulation or upon birth. Spatial coordinates represent the individual's position on the raster map, defined by the row and column numbers. The age of individuals ranges from zero (individuals less than one year old) to the maximum lifespan, which is determined by the life history traits of the species. The breeding-state variable includes three categories: non-breeder, breeder, and chick. Energy (*E*) represents the energetic state of non-breeding and breeding individuals and is updated at each time step according to Equation 1 (Table 1). In this equation, *C* represents the energy consumption from foraging, *B* is the fixed energy lost through basal metabolism (denoted as βbasal), *M* is the energy expended through movement (calculated as βloss × movement distance), and *R* is the energy allocated to reproduction. Reproductive energy (*R*) includes the constant energy required for offspring production and its supply throughout the breeding season (denoted as βsupply). For simplicity, chick energy expenditure is not modeled explicitly. Fledging probability is determined by parental provisioning, as described in the Reproduction sub-model.

The energy raster representation of the environment consists of a 21 × 21 grid, arranged with a toroidal (donut-shaped) topology. This means that when an individual crosses the grid's boundary, it reappears at the opposite edge, avoiding potential artifacts due to spurious edge effects. Each cell in the grid is assigned an energy value, expressed in kilojoules (KJ), and the cell's position is defined by its column and row numbers. Energy values are drawn from a zero-inflated negative binomial distribution (ZINBI; Rigby et al., 2019), providing variability in the energy content across the grid (Figure 1). The colony is positioned at the center of the grid, with coordinates (xcord, ycord) = (10,10) (Figure 1). The trap raster is defined by the presence or absence of a trap in each cell, with its layout also determined by the grid's column and row coordinates (Figure 1).

A year is represented as 365 days in the model, with each simulation step corresponding to 6 hours. As such, each day is composed of 4 steps, and a full year consists of 1460 steps. The model does not incorporate a circadian rhythm but includes seasonality, with distinct breeding and non-breeding periods. The breeding period is divided into two phases: the 'laying window,' during which individuals

produce offspring within the colony, and the 'fledging period,' in which parents commute between the sea and the colony to feed their chicks until they fledge or die. In our model, we represent a typical seabird phenology, with a breeding period lasting 146 days. This includes a 20-day 'laying window' for egg-laying and a 126-day 'fledging period,' which is consistent with the mean lengths of the incubation and fledging periods observed in seabird species (Schreiber and Burger, 2001).

2.4. Process overview and scheduling

The general schedule of the program is described in Figure 2. The program begins by defining the initial conditions, including the collection of individuals, their memory, and their state variables, the environment (energy raster), and the trap scenario. Afterward, the model begins to operate. Within each time step (6 hours), seven main sub-models or modules are processed in the following order: (1) Energy update, (2) Movement, (3) Trap mortality, (4) Reproduction, (5) Mortalities, (6) Updates and (7) End simulation.

In the Energy update sub-model, the energy of the environment and the subsidy are replenished (see Energy update sub-model). Next, the Movement and Foraging sub-model operates, and birds rest, feed (consume energy), or move (random walk or 'oriented' random walk) based on their hunger level (i.e., energy level, see 'Movement and Foraging' sub-model). In the Trap Mortality module, deaths due to trap interactions are evaluated. Following this, the Reproduction sub-model operates. Satiated non-breeders who meet the breeding conditions during the laying window will go to the colony and produce offspring (see 'Reproduction' sub-model). During the fledging period, satiated breeders return to the colony to feed their chicks and will continue to do so until the chick fledges or dies (see 'Reproduction' sub-model). In both cases, once this occurs, the breeders transition to non-breeder status. The same applies at the end of the fledging period for unsuccessful breeders (those whose chicks did not fledge). Next, the Mortalities sub-model operates, and death probabilities are assessed due to starvation, age, and other constant mortality factors (see 'Mortalities' sub-model). At the end of the algorithm, the age, energy, and memory of individuals are updated. The basal energy expenditure ($\beta basal$) and the energy lost due to movement ($\beta loss \times$ movement distance) are subtracted from the individuals' energy reserves.

The memory is then updated to store the coordinates and respective foraging success of each individual's current cell. Subsequently, for each individual, the cells in their memory are arranged from

highest to lowest foraging success, and the first n = βmemory cells are stored. Individuals retain their memory throughout their lifetime. Lastly, the simulation stops either when the last iteration is reached or if the population becomes extinct. In both cases, the program saves the output.

2.5. Design concepts

2.5.1. Basic principles

This model is built on the assumption that seabird populations are food-limited and energetically enriched habitats (trophic subsidies) generate benefits for foraging and reproduction, but they also increase the risk of mortality. Consequently, population vital rates respond in opposite directions to habitat selection. The model is based on animals' ability to make behavioral and reproductive decisions using their previous foraging experience and current condition (energy). For instance, birds decide when to leave their present patch, in which direction to move, or when to go to reproduce in the colony.

2.5.2. Emergence

Population size emerges as the result of individuals' foraging success, survival, and reproduction within a patchy and dynamic environment with limited resources. Movement is guided by a combination of experience and randomness. Reproduction is influenced by probabilities weighted by foraging success and life history traits. Mortality rates are determined by the combination of foraging success, age-specific mortality curves, and interactions with the environment (including trap mortality). As such, population growth is not directly modeled but emerges from the interplay of these factors within the simulation.

2.5.3. Adaptation

Individuals follow spatially explicit movement rules, guided by their hunger (energy level) and previous foraging experience, to locate food patches.

2.5.4. Learning

Individuals remember the locations of previously visited cells and the duration of successful foraging there (foraging success is defined as the cumulative time spent in a cell where consumption exceeds 95% of the maximum possible consumption, i.e., βhunger). As individuals age, they accumulate foraging experience and, on average, spend more time in higher-quality patches. Individuals do not learn from others' experiences, relying solely on their own interactions with the environment.

2.5.5. Prediction

Individuals determine their movement direction based on the quality of habitats where they have previously foraged. These decisions are made without estimating future conditions or the consequences of their actions. As a result, individuals rely solely on past experiences to guide their foraging behavior.

2.5.6. Sensing

Individuals know their present location, energy level, and memory. Based on these traits and seasonality, they can modify their behavior (as explained in the sub-model section). Individuals do not identify the habitat of their neighboring cells, nor do they recognize emergent properties of the population, such as its size (whether at sea or in the colony).

2.5.7. Interaction

The model simulates an environment with limited energy, where exploitation competition is the primary form of indirect interaction. There are no hierarchical structures governing habitat selection or food consumption among individuals. Additionally, individuals do not assess the number of others in the same cell, nor can they predict the potential future locations of other individuals, which may influence their movement decisions.

2.5.8. Stochasticity

Randomness in the model is incorporated through probabilities in individual movement decisions, reproduction, mortality, and energy renewal from the environment. Individuals without foraging experience follow a random walk pattern. Birds with prior experience in high-quality cells use weighted probabilities, based on their experience, to move towards those areas rather than following a straight-line path. Reproduction events (both laying and fledging) and mortality events (age-related, trap-related, starvation, and constant mortalities) are determined by weighted probabilities. The energy content of each cell changes dynamically over time, adding an additional layer of unpredictability.

2.5.9. Collectives

Individuals do not form or belong to aggregations that influence each other's behavior or decisions. Each individual's actions are independent of others, and there are no social dynamics affecting habitat choice, foraging, or reproduction.

2.5.10. Observation

At the end of each simulation, population-level variables were recorded, including total population size, number of newborns, recruits (breeders and chicks), and deaths, categorized by cause.

2.6. Initialization

Prior to each simulation, 180 individuals were randomly distributed across the environment, all assigned a non-breeding status. The ages of individuals were randomly drawn from the age distribution of populations under stationary growth conditions (90–100 years in control conditions) for each life-history type, based on prior model runs. The individuals' energy levels followed a normal distribution with a mean of βhunger ± 10 SD. At the beginning of the simulation, individuals had an 'empty' memory. The energy content of each cell was randomly sampled from a ZINBI distribution and scaled by the parameter βfood to reach the desired population size. The spatial configuration of the trap was defined by the corresponding trap parameters (Table 2).

2.7. Sub models

This section provides a detailed description of the sub-models for Energy update, Movement and Foraging, Trap Mortality, Reproduction, and Mortalities (Figure 2).

2.7.1. Energy update sub-model

When the energy of a cell decreases to a minimum value due to consumption by individuals, it begins to increase proportionally to its initial value following a logistic replenishment function (see equations 2 and 3, Table 1). In this function, replenishment steps[i,j] denotes to the number of time steps elapsed since replenishment began for cell [i, j]. The parameter βreplenishment defines the midpoint (x-value) of the logistic curve, and k represents the steepness of the curve (with k = 1).

In this sub-model, the energy from the subsidy (βsubsidy) is subsequently added to the cells where the trap is located. The amount of energy added depends on the trap parameters defined in the experiment (see Table 2).

2.7.2. Movement and Foraging sub-Model

This sub-model simulates the movement and foraging behavior of individuals within a one-step period (6 hours), considering their energy levels and decision-making processes (Figure 2). During each simulation step, birds either rest, feed, or move, depending on their hunger level. If a bird is not hungry (energy > βhunger), it remains in the same location and rests. If it is hungry (energy < βhunger), it attempts to consume energy in its current location. Energy consumption is modeled using a two-parameter Holling Type II response (Holling, 1959), commonly applied to approximate feeding behaviors observed in nature (Sibly et al., 2013), as shown in Equation 4 of Table 1. In this equation, βhunger represents the maximum energy consumption in kilojoules (KJ), energy[i,j] is the amount of energy available in the current cell, and βholling is the half-saturation constant that controls the rate at which energy consumption approaches its maximum as available energy increases. Energy consumption by individuals in the same cell occurs sequentially (using a for-loop) and in random order, with no hierarchical structure among individuals. Following the marginal value theorem, individuals leave the current cell when their consumption drops below a certain threshold (Charnov, 1976). In contrast to the marginal value theorem, which defines this threshold relative to the habitat, our model assumes that individuals base this decision on their own energetic state. Specifically, they leave the current cell when the energy they consume falls below or equals their basal energy expenditure (parameter βbasal).

For modeling movement, birds follow a memory-biased random walk, directing their movement toward previously successful foraging locations. The only exception is recruits leaving the colony, who lack prior experience and thus follow an unbiased random walk. These naïve birds move to a neighboring cell within their movement radius (βradius), following a modified random walk pattern in which diagonal movement is penalized by a factor of 0.7 to maintain an isotropic movement pattern. All other birds (i.e., those with at least one memory cell), bias their movement toward the cell where they previously had the greatest foraging success. In these cases, the probability of moving to a given cell within their movement radius is determined by a logistic function that regulates the degree of directional stochasticity, based on the parameters βkdire and βdire (see Figure S1). This function allows birds to be guided toward a preferred direction while retaining flexibility to deviate from a straight-line path (see Figure S2).

To compute directionality, we first calculate the direction vector from the preferred cell to each candidate neighboring cell ($dire_{pref}$, Equation 5 Table1). We then calculate the direction vector from the current cell to each candidate ($dire_i$, Equation 5 Table1) cell. The absolute angular difference between these two vectors is computed (Equation 5, Table 1) and passed through a logistic function to assign weights to each candidate cell (Equation 6, Table 1). In this function, βdire sets the midpoint and βkdire the steepness of the curve, thus regulating how strongly birds are biased toward the preferred direction. Higher βdire and lower βkdire values result in more stochastic movement.

Finally, cell selection is implemented through weighted random sampling based on Equation 7 (Table 1), where Cell $weight_i$ is the weight assigned to cell *i,* $\sum_{j=1}^{n} P_j$ is the total sum of weights across all candidate cells, and *n* is the total number of cells within the movement radius. For unbiased movement (i.e., naïve individuals), the same formula is applied, assigning an equal weight of 1 to all candidate cells—except diagonals, which are penalized with a weight of 0.7 to maintain isotropic movement.

2.7.3. Trap-mortality sub-model

In this sub-model, the probability of mortality for individuals located in trap cells (trap raster) is assessed. The trap lethality parameter (βlethality) is compared to a random sample drawn from a uniform distribution between 0 and 1 (U). Mortality occurs when β lethality > U resulting in a probability of one. Otherwise, the probability is zero (see, Equation 8, Table 1). The same uniform random variable U is used consistently throughout the following sub-models to represent stochastic processes.

2.7.4. Reproduction sub-model

This sub-model simulates the reproduction process of seabirds during the breeding season, including chick production during the 'laying window', provisioning by the parents, and the fledging of chicks. For simplicity, the model treats birds as asexual organisms. Reproduction depends on the age of first reproduction (βfirstbreed) and the individual's current (βhunger) and wintering (βreproduction) energetic condition. The energetic condition during wintering is evaluated using a logistic function based on the number of time steps in which the individual was satiated during the non-breeding season. If the output of this function exceeds a random value drawn from a uniform distribution (U), the individual is considered to have wintered successfully, as shown in Equation 9 in Table 1. In this equation, βreproduction defines the midpoint (x-value) of the logistic function, and *k* represents the steepness of the curve (*k = 1*). In addition to a successful wintering outcome, a bird can reproduce

during the laying window if it meets two further conditions: it must be at or above reproductive age (age ≥ βfirstbreed) and its energy level must exceed the required threshold (energy> βhunger). If these conditions are met, the bird moves to the colony in a straight line over one time step and produces n=βclutch number of chicks. When reproduction occurs, the 'mother' loses a fixed amount of energy (βsupply), and the chick(s) gain the same amount of energy (βsupply).

During the 'fledging period,' chick provisioning is based on the hunger parameter (βhunger). Once satiated, the breeder returns to the colony in a straight line over one time step, regardless of their location, to supply the chicks. For simplicity, the model does not explicitly simulate the various activities of birds during the reproductive stages, such as incubation, brood-guarding, or creches. Chicks are fed a fixed amount of energy throughout the reproductive stage, equivalent to the supply parameter (βsupply), while the 'mother' loses a constant amount of energy (βsupply). Chick fledging is modeled as a probabilistic event governed by a logistic function based on the number of times a chick was fed by its parent. If the output of this function exceeds a random value drawn from a uniform distribution (U), the chick is considered to have successfully fledged, as shown in Equation 10 in Table 1. In this equation, βfledge denotes the midpoint (x-value) of the logistic function and k determines the steepness of the curve (set to 1). Once fledging occurs, chicks transition to non-breeders and their energy is reset to the hunger parameter (βhunger).

2.7.5. Mortalities sub-model

In this sub-model non-trap related mortalities are evaluated, including starvation, age-dependent, and constant mortalities.

Starvation mortality: Starvation mortality is evaluated at each time step using a logistic function based on the accumulated number of time steps during which an individual has not consumed energy—either through foraging (in the case of adults) or provisioning (in the case of chicks). If the output of this function exceeds a random value drawn from a uniform distribution (U), the individual dies from starvation, as shown in Equation 11 in Table 1. In this equation, βstarvation represents the midpoint (x-value) of the logistic function, and k controls its steepness (fixed at 1).

Age-dependent mortality: The probability of mortality due to age is assessed every five days and is estimated using a three-parameter exponential decay function based on the individual's age. If the output of this function exceeds a random value *U*, the individual dies, as shown in Equation 12 in Table

1. In this equation, βmin is the minimum mortality rate, βmax is the maximum mortality rate, and βdecay controls the rate of exponential decline in mortality with age. By adjusting βmin and βmax, we define age-dependent mortality curves for each life history, using a consistent decay rate (βdecay = 5). Additionally, individuals die when they reach the maximum age (βsenescence) specific to their life history.

Constant mortality: This is a fixed probability of death, assessed once per year during the first step of each year. If the constant mortality parameter exceeds a random value U, the individual dies, as shown in Equation 13 in Table 1. In this equation, βconstant is the fixed mortality probability applied uniformly across all individuals during the annual mortality check.

2.8. Calibration and parameterization

The parameters used in the model are presented in Table 2. We calibrated the parameters as follows: First, we set the basal expenditure parameter (βbasal) according to the average ratio between the field metabolic rate (FMR) and the basal metabolic rate (BMR) in seabirds, i.e., βhunger/3.5 (Schreiber and Burger, 2001). Subsequently, we calibrated the βhunger parameter so that, during the non-breeding season, individuals consumed an amount equivalent to the FMR of an average seabird (800 grams), following an allometric function of $16.69 \times \text{mass}^{0.651}$ (Schreiber and Burger, 2001).

Considering the energy replenishment parameter, individuals fed most frequently 1 or 2 times per day and consumed an average of 1200 KJ per day. Seabirds tend to increase their FMR throughout the breeding season, from incubation to brood to creche (Dunn et al., 2018). Accordingly, the parameter for energy loss from movement (βloss) was calibrated so that birds increased their average daily consumption by approximately 40% during the breeding season (~1600 KJ/day), due to the cost of commuting between the colony and the foraging grounds.

The movement radius was calibrated to allow individuals to reach the "edge" of the environment—used as a reference point in the toroidal landscape—within one day (four steps). The parameters regulating movement stochasticity (βkdire and βdire, Table 2) were adjusted to balance randomness in movement while minimizing the risk of frequent starvation-related mortality (see, Figure S1, S2).

We set the Holling type 2 constant (βholling) so that the function reaches half of its maximum value when the energy available to an individual equals the maximum consumption (i.e., βhunger). The parameter for the energy cost of chick production and chick supply (βsupply) was established at 10%

of the βhunger parameter. This represents an intermediate cost, considering that for most of the nestling period, seabird parents deliver meals weighing 5 to 35% of the adult body mass (Schreiber and Burger, 2001).

Based on the parameters described above, chicks were fed most frequently one to two times per day. This feeding frequency falls within the range typical for seabirds provisioning their chicks, with variations ranging from several meals a day to one every one or two days. Consequently, we adjusted the fledging parameter to ensure that chicks fed at least once a day had a high probability of fledging. The parameter for starvation mortality was determined based on the allometric starvation model for an average seabird, following the approach of (Peters, 1983).

We calibrated the energy distribution parameters of the raster (ZINBI distribution, βmu, βsigma, βnu) to achieve a high degree of patchiness while minimizing frequent deaths among individuals under control conditions (see above). The selected distribution included 40% zeros and ranged from 0 to 12 units (KJ).

We parameterized three life histories—slow, intermediate, and fast—based on typical reproduction and survival traits in seabirds following Schreiber and Burger, (2001), including mean clutch size, age at first reproduction, age-specific mortality, and senescence. As a reference, we used the parameters of an average albatross for the slow species, a seagull for the intermediate species, and a cormorant for the fast species (Table 2).

2.9. Experiments

We first developed a base trap configuration to evaluate the effects of compensatory ecological traps on seabird populations. This model focused on a trap placed in the highest-quality habitat and served as the reference for all subsequent analyses (Figures 1 and 3). From this base, we implemented three additional trap configuration variations to explore the influence of trap area and spatial distribution. Combining the four trap configurations with three levels of bycatch mortality and three levels of trophic subsidy resulted in a total of 36 unique simulation scenarios. Below, we detail the structure and assumptions of the base model, followed by a description of the additional configurations.

The base trap configuration featured a compensatory trap located in a high-quality area—randomly selected from cells within the 90th percentile of energy values. This trap occupied 15% of the habitat, remained present year-round, and added a daily trophic subsidy to the environment. Such traps may

be common in marine predator-fishery interactions, as both predators and fisheries tend to co-occur in highly productive areas, including mesoscale frontal systems, eddies, upwelling zones, and continental shelves (Karpouzi et al., 2007; Scales et al., 2018; Welch et al., 2024). Simulations ran over a 100-year period, beginning with a 24-year initial phase during which populations were allowed to reach stable equilibrium (the 'control condition'). In year 25, the compensatory trap was introduced. We defined three levels for both mortality and subsidy—low, medium, and high. Preliminary analyses of population responses to a mortality gradient revealed that life histories tend to converge at both extremes of mortality. Therefore, we set intermediate, realistic values (with realized mortality ranging from 2% to 23%) where the differences among life histories were more pronounced (Table 2). We defined subsidy levels at which populations reached 1, 2, and 3 times the carrying capacity under control conditions without trap mortality.

Given the distinct life histories of the species and the sources of stochasticity, populations reached different equilibrium sizes (slow < intermediate < fast). To allow comparison across replicates, population sizes were standardized by their average equilibrium values. We then assessed short- and long-term population responses to the compensatory trap. The short-term response was measured as the average standardized population size during the first 10 years after the trap's introduction, while long-term response was measured as the average standardized population size over the last 10 years of the simulation.

To evaluate the effects of trap configuration, we modified the base configuration to include three additional variations (1) a larger-area trap, covering 25% of the habitat; (2) a smaller-area scenario trap, covering 5% of the habitat; and (3) a randomly distributed trap covering 15% of the habitat (Figure 3). For these variations, we analyzed only the long-term responses in comparison to the base model. Unless otherwise stated, results are expressed as means ± one standard deviation (SD).

3. Results

3.1. Base trap configuration

Population responses to the nine compensatory trap scenarios under the base configuration over a 100-year simulation period are shown in Figure 4. Below, we describe in detail the short- and long-term dynamics for each of the three life-history strategies (Figure 5).

Slow Species (e.g., albatross): At low mortality, the slow species maintained a population size similar to the control under low subsidy (Figure 5a) and exhibited slight growth at medium (1.1 ± 0.14 times control) and high subsidy (1.1 ± 0.09 times control) levels in the short term (Figure 5a-c). However, in the long term, the population declined as subsidy levels increased (Figure 5a-c), reaching 0.3 ± 0.09 times the control population under high subsidy (Figure 5c). At medium mortality, the slow species experienced a more pronounced short-term decline, which intensified with higher subsidy levels (from 0.86 ± 0.05 times control at low subsidy to 0.76 ± 0.1 times control at high subsidy, Figure 5d-f). Ultimately, this led to extinction across all subsidy levels in the long term (100% probability, Figure 5d-f). Under high mortality, the slow species showed an even steeper short-term decline as subsidy levels increased, resulting in a 100% probability of extinction (Figure 5g-i).

Intermediate Species (e.g., gull): At low mortality, the intermediate species achieved slightly higher asymptotic growth than the control in the long term (1.1 ± 0.02 times control, Figure 5a). At medium and high subsidy levels, it attained more substantial asymptotic growth, reaching 1.7 ± 0.09 and 2.6 ± 0.1 times the control, respectively (Figure 5b-c). Under medium mortality, the intermediate species exhibited a non-linear short-term response, peaking at medium subsidy levels (1.1 ± 0.12 times control, Figure 5e-f). However, in the long term, it showed lower asymptotic growth than the control at low subsidy (0.7 ± 0.19 times control, Figure 5d) and faced a tendency toward decline and eventual extinction at intermediate and high subsidy levels, with 43% and 71% probabilities of extinction, respectively (Figure 5e-f). Under high mortality, the intermediate species experienced sharp short-term declines and ultimately reached a 100% probability of extinction in the long term (Figure 5g-i).

Fast Species (e.g., cormorant): At low mortality, the fast species grew rapidly in the short term and reached asymptotic growth in the long term, attaining 1.3 ± 0.05, 1.8 ± 0.04, and 2.7 ± 0.09 times the control size as subsidy levels increased from low to high (Figure 5a-c). Under medium mortality, the fast species exhibited a non-linear short-term response similar to that of the intermediate species, with its highest population size observed at medium subsidy (1.4 ± 0.09 times control, Figure 5d-f). In the long term, it reached asymptotic growth at 1.2 ± 0.06 and 1.6 ± 0.16 times the control as subsidy levels increased from low to medium. At high subsidy, it grew to a larger size, but without reaching asymptotic growth (2.3 ± 0.28 times control, Figure 5f). Under high mortality, the fast species initially matched control population sizes at low and medium subsidy levels but experienced a short-term decline at high subsidy (0.8 ± 0.11 times control, Figure 5g-i). In the long term, it stabilized at sizes similar to the control

458 under low subsidy (0.9 ± 0.11 times control, Figure 5g), while the likelihood of decline increased at
459 medium and high subsidy levels, reaching 29% and 100% probabilities of extinction, respectively (Figure
460 5h-i).

461 **3.2. Trap variations**

462 The smaller-area trap increased the resilience of declining populations compared to the base model
463 and reduced the carrying capacity (K) for growing populations (Figure 6). In contrast, the larger-area
464 trap generally had more severe impacts on declining populations and increased K for growing
465 populations compared to the base model (Figure 6). Overall, the random trap scenario was less severe
466 for declining populations and also increased K for growing populations in comparison to the base model
467 (Figure 6).

468 **4. Discussion**

469 Understanding the mechanisms behind ecological traps is essential, especially given the rapid,
470 human-induced environmental changes that present poorly known risks to populations. Previous
471 ecological trap models have generally assumed reduced survival and/or reproduction among trapped
472 populations (Battin, 2004), leading to the conclusion that these traps inevitably decrease population
473 sizes and heighten vulnerability to stochastic extinction. Our model introduces a novel trade-off:
474 increased recruitment—driven by trophic subsidies—counterbalanced by a reduction in survival rates.
475 While the model predicts similar results to previous models, it also reveals critical differences. As
476 expected, the severity of trap impacts increases when traps occupy larger portions of available habitats
477 or when they emerge in higher-quality habitats that attract greater preference (Delibes et al., 2001;
478 Fletcher et al., 2012; Hale et al., 2015). Below, we explore novel aspects of our model predictions, the
479 assumptions underpinning them, areas for future refinement, and contrasts with existing evidence of
480 seabird-fishery interactions. Finally, we discuss their implications for effective management and
481 conservation strategies.

482 **4.1. Fitness trade-offs within the ecological trap framework**

483 Our model revealed a critical interaction between trophic subsidies and mortality, resulting in more
484 complex population responses than anticipated by previous ecological trap models. These included
485 non-linear responses both over time and across different levels of subsidy and mortality. All three life
486 histories displayed non-linear temporal dynamics, where the initial positive effects of recruitment

(breeders and fledging, Figure S3, S4) outweighed mortality (Figure S5). However, populations were unable to sustain growth in the long term, leading to eventual declines (e.g., the slow-lived species in scenario C, the intermediate-lived species in scenario E, and the fast-lived species in scenario G, Figure 4). This highlights the challenge of detecting a trap that appears advantageous in the short term but can lead to long-term population extinction. Overall, these responses are expected to be more common in fast-lived species, as they have greater potential for population growth, which also implies more pronounced density dependence (Herrando-Pérez et al., 2012), higher demographic stochasticity (Sæther et al., 2004) and a greater tendency toward nonlinear and chaotic dynamics (Clark and Luis, 2020; Rogers et al., 2022).

Similarly, all three life histories exhibited non-linear responses across varying levels of mortality and subsidy. At lower mortality levels, trophic subsidies effectively compensated for mortality and promoted population growth. However, once mortality exceeded a critical threshold, subsidies amplified mortality impacts—specifically, increased habitat preference elevated effective mortality (Figure S5)—ultimately causing population declines and, in some cases, extinction. In contrast, simulations by Hale et al., (2015) showed that reductions in either fecundity or survival within traps individually decreased metapopulation persistence, but their combined effects did not further amplify trap impacts. Our findings emphasize the importance of incorporating trade-offs among fitness components into ecological trap frameworks (Battin, 2004), as habitat preference can cause fitness components to respond antagonistically or synergistically, resulting in more diverse responses than those anticipated by ecological trap models.

4.2. Influence of life history on compensatory ecological traps

Additionally, our results demonstrate that the interplay between mortality and subsidies is heavily influenced by species' life history traits along the slow-fast continuum (Saether, 1987)—the main axis of life history variation across several taxa, including mammals, birds, reptiles, fishes, insects, and plants (Capdevila et al., 2020; Cooney et al., 2020; Gaillard et al., 2016; Sibly et al., 2012). Considering the three habitat preference scenarios (base, higher, and lower area), our model predicts that the species with the slowest life history is 1.41 and 4.5 times more likely to face extinction compared to species with intermediate and fast life histories, respectively. These findings align with theoretical expectations, highlighting that 'slow' life-history species are particularly vulnerable to local extirpations caused by traps (Hale et al., 2015). In contrast, faster species exhibit greater resilience and, under similar

conditions, can thrive, with population sizes potentially increasing up to threefold compared to control groups. These results suggest that compensatory traps may amplify the selective filtering of life history more intensely than previously anticipated (Hale et al., 2015; Kokko and Sutherland, 2001).

Recent studies within a broader context agree with our findings, indicating that species with longer generation times require extended recovery periods following disturbances, while species with shorter generation times tend to exhibit greater resilience (Capdevila et al., 2022). Furthermore, animals with slower life histories are generally at greater risk of extinction compared to faster-reproducing species, including plants, mammals, birds, reptiles, amphibians, and freshwater fish. This could result in big shifts in ecological strategies across the tree of life (Carmona et al., 2021; Cooke et al., 2019; Richards et al., 2024, 2021). Integrating various trade-offs between fitness components into the theoretical framework of ecological traps is thus essential for identifying traps and clarifying their contribution to the global filtering of animal life histories.

4.3. The case of seabirds-fisheries interaction

Model predictions agree with previous research documenting a variety of responses in seabirds across the slow-fast continuum in relation to fisheries discards and bycatch. For instance, studies on slow species such as albatross and shearwater suggest that while fisheries subsidies can enhance reproductive traits like recruitment and breeding success, these gains are offset by reduced survival rates due to bycatch, ultimately causing important population declines (Cleeland et al., 2021; Genovart et al., 2017, 2016; Pardo et al., 2017; Rolland et al., 2010, 2009, 2008; Tuck et al., 2015; Véran et al., 2007). A well-documented case in South Georgia illustrates the impact of bycatch on the wandering (*Diomedea exulans*), gray-headed (*Thalassarche chrysostoma*), and black-browed (*Thalassarche melanophris*) albatrosses. Despite potential reproductive and recruitment increases from fishery discards, bycatch has led to drastic declines in these populations, estimated at 40–60% over the past 35 years (Pardo et al., 2017). Similarly, the Balearic shearwater (*Puffinus mauretanicus*), Europe's most endangered seabird, has experienced substantial population declines due to bycatch. Projections suggest that, if bycatch rates remain unchanged, this species could face extinction within the next 61 years (Genovart et al., 2016). These findings are reinforced by recent studies that seabird life history traits predict extinction risk and vulnerability to anthropogenic threats, including bycatch (Richards et al., 2024, 2021).

In contrast, for species with fast life history traits our model predicts greater resilience and even potential for population growth in response to compensatory traps. Discards can positively influence various reproductive traits of faster seabirds (Oro et al., 2013), which often demonstrate greater phenotypic plasticity in reproduction compared to slower species. These species, which lay up to six eggs (Schreiber and Burger, 2001), show earlier laying dates, increased clutch sizes, and improved hatching and breeding success. Notable examples include Audouin's gull (*Larus audouinii*), the Yellow-legged gull (*Larus cachinnans*), and the Lesser Black-backed gull (*Larus fuscus*) (Oro, 1996; Oro et al., 1996, 1995). Studies have shown a positive correlation between subsidy availability and population size, as well as a negative correlation with population variability in these gull species. This suggests that subsidies can mitigate the high demographic stochasticity inherent to fast life histories (Oro et al., 2013). Surprisingly, evidence for the positive effects of fishery discards on seabird population sizes remains largely circumstantial. Most such evidence stems from Northern Hemisphere seabirds, including black-backed gulls (*Larus marinus*), herring gulls (*Larus argentatus*), great skuas (*Stercorarius skua*), northern gannets (*Morus bassanus*), and northern fulmars (*Fulmarus glacialis*). These species experienced rapid population growth during the peak of discard production in the 20th century but have since stabilized or declined (Bicknell et al., 2013; Langlois Lopez et al., 2023; Oro et al., 2013; Wilhelm et al., 2016). While current fishery discards are approximately half of 1980s and 1990s levels, recent estimates suggest that global fisheries still discard between 7 and 16 million tons annually, with nearly 60% originating from trawl fisheries (Gilman et al., 2020). This substantial volume of discards likely continues to sustain large seabird populations. For instance, one extensive study found that despite a 48% decrease in North Sea discards from 1990 to 2010, these discards still supported an estimated 3.3 to 9.7 million seabirds annually (Sherley et al., 2019). These findings highlight the urgent need to reduce uncertainties surrounding global discard estimates and to investigate their role in driving compensatory traps for seabirds.

4.4. Model assumptions, caveats, and future improvements

Our model was based on two key assumptions. First, we assumed that populations were energetically limited. Second, we assumed that species with different life histories were approximately bioequivalent, meaning that they acquire and use energy in the same way, sharing all parameters except for life history. This assumption meets with the "energy equivalence rule," a central principle of the metabolic theory of ecology (Brown, 2004; Robert Burger et al., 2021), which posits that energy

partitioning among species in space is independent of body mass, due to compensatory variation in metabolism-mass and abundance-mass relationships (Hatton et al., 2019). However, evidence from birds suggests that "population metabolism" (i.e., the total amount of basal energy used by a population per unit area) tends to be higher in larger species (Hatton et al., 2019), implying that compensatory effects may be smaller for slower species than predicted by our model. Nevertheless, if the assumption of bioequivalence does not hold, compensatory traps could lead to population responses that are difficult to predict. Such responses might include changes in habitat use, vital rates, population growth rates, and overall population sizes.

Additionally, to simplify our model, we assumed identical reproductive phenology across life histories. This assumption allowed us to evaluate traps with equal exposure for all life histories, but it may overlook critical aspects of life-history variation. For example, the duration of the developmental period is a fundamental axis of life-history variation (Cooney et al., 2020). Differences in developmental times, and consequently in the use of parental habitat, could influence species' responses to ecological traps, potentially leading to disparities in trap exposure and severity.

Finally, our model follows the principles of optimal foraging theory, which suggests that individuals make foraging decisions aimed at maximizing their fitness. Decisions about when and where to move are influenced by both hunger and previous foraging success. A valuable enhancement would be to incorporate trade-offs into these decisions (Railsback, 2022), such as those between hunger and fear, or by using more direct fitness measures, including growth, survival, reproduction, and risk avoidance. Incorporating fear, in general terms, is expected to increase species resilience. However, how fear emerges in response to the accumulated experiences of different life history strategies and its population-level consequences remain intriguing avenues for future research.

4.5. Management implications

Our study suggests that compensatory trap models could be essential for understanding and predicting the impacts of anthropogenic food subsidies—such as crops, dumps, restaurants, offal, and fisheries discards—on scavenger species (Munstermann et al., 2022; Oro et al., 2013). These subsidies often come with major fitness costs, including increased risks of poisoning, pathogen infection (e.g., in birds: Becker et al., 2015), interference competition (e.g., in sharks: Semeniuk and Rothley, 2008), predation (e.g., in mammals and birds, Morris, 2005; Rodewald et al., 2011), hunting (e.g., mammals,

Simon and Fortin, 2020), and incidental mortality (e.g., in seabirds, turtles, marine mammals and elasmobranchs: Lewison et al., 2014).

Ecological trap models have evolved from basic source–sink frameworks to more realistic individual-based models (IBMs) that incorporate habitat selection, learning and adaptation, local interactions (both spatial and social), and dynamic, heterogeneous environments. These models have been increasingly applied in terrestrial ecosystems, offering valuable insights for management and conservation (Sánchez-Clavijo et al., 2016; Simon and Fortin, 2020). In contrast, their application in marine systems remains limited, despite growing empirical evidence of their relevance (Swearer et al., 2021). In seabird–fishery interactions, for example, trap frameworks have mostly focused on fitness declines due to low-quality prey—an idea captured by the "junk food hypothesis" (Grémillet et al., 2008). Our findings, together with previous studies (ACAP, 2024; Favero et al., 2011; González-Zevallos and Yorio, 2006; Sullivan et al., 2006; Watkins et al., 2008), underscore the urgent need to recognize compensatory traps as an unintended consequence of fisheries. These traps should be considered a cornerstone for advancing ecosystem-based fisheries management (EBFM) (Pikitch et al., 2004).

Integrating compensatory trap models into EBFM frameworks could substantially enhance conservation and management outcomes. These models could complement current population risk assessments—such as those endorsed by ACAP—which often overlook the interactive effects of trophic subsidies and bycatch. Parametrized using seabird movement and behavior (www.seabirdtracking.org, Carneiro et al., 2024), metabolism (Dunn et al., 2018; Sibly et al., 2013), and demographic and fisheries data (e.g., bycatch rates and discard energy from observer programs), these models can help establish clear management objectives and fishery-specific thresholds. In doing so, they can identify sustainability tipping points—conditions under which subsidies shift from buffering to amplifying bycatch impacts—thus informing discard regulations and long-term mitigation strategies.

5. Conclusion

Our model reveals a critical interaction between subsidies and mortality, with species-specific thresholds along the slow–fast life-history continuum. These thresholds mark the point at which subsidies switch from conferring demographic benefits to producing negative synergistic effects with mortality, as stronger habitat preference increases exposure to lethal conditions. Under comparable behavioral and metabolic settings, slow-lived species are most vulnerable to extinction in

compensatory traps—~1.4× more likely to go extinct than intermediate-lived species and ~4.5× more likely than fast-lived species—whereas fast-lived species exhibit greater demographic resilience and can even grow under some regimes. These results support and extend ecological-trap theory, underscoring the need to broaden the framework to explicitly accommodate fitness trade-offs across vital rates. By clarifying how trophic subsidies and mortality interact across life-history strategies, our work identifies when traps emerge and how they filter species by strategy, shaping population dynamics. Importantly, the findings call for integrated management of bycatch and discards: their demographic effects are interdependent and can jointly reinforce maladaptive habitat selection, elevating extinction risk. In these contexts, compensatory traps offer a mechanistic, decision-relevant framework for advancing ecosystem-based fisheries management (EBFM) and improving conservation outcomes

659 **Tables**

660 Table 1. Summary of the equations used in the simulation model. Symbols and parameter definitions
661 are provided in the main text.

	Equation	Sub model
Eq. 1	$E_{(t)} = E_{(t-1)} + C - B - M - R$	Movement and Foraging / Reproduction / Updates
Eq. 2	$\text{Energy}[i,j] = \text{Energy initial}[i,j] \times \text{Prop(replenishment)}\ [i,j]$	Energy update
Eq. 3	$\text{Prop(replenishment)}\ [i,j] = \frac{1}{1 + e^{k(\text{replenishment steps}[i,j] - \beta\text{replenishment})}}$	Energy update
Eq. 4	$\text{Consumption} = \beta\text{hunger} \times \frac{\text{energy}[i,j]}{\text{energy}[i,j] + \beta\text{holling}}$	Movement and Foraging
Eq. 5	$\text{diff} = 180 - \lvert\lvert \text{dire}_{\text{pref}} - \text{dire}_i \rvert - 180\rvert$	Movement and Foraging
Eq. 6	$\text{Cell weight} = \frac{1}{1 + e^{\beta k \text{dire}(\text{diff} - \beta\text{dire})}}$	Movement and Foraging
Eq. 7	$P(c_i) = \frac{\text{Cell weight}_i}{\sum_{j=1}^{n} P_j}$	Movement and Foraging
Eq. 8	$[\text{trap mortality}] = \begin{cases} 1, & \text{if } \beta\text{lethality} > U \\ 0, & \text{otherwise} \end{cases}$	Trap-mortality
Eq. 9	$[\text{successful winter}] = \begin{cases} 1, & \text{if } \frac{1}{1 + e^{k(\text{satiated steps} - \beta\text{reproduction})}} \\ 0, & \text{otherwise} \end{cases}$	Reproduction
Eq. 10	$[\text{fledgling}] = \begin{cases} 1, & \text{if } \frac{1}{1 + e^{k(\text{provisioning events} - \beta\text{fledge})}} > \\ 0, & \text{otherwise} \end{cases}$	Reproduction
Eq. 11	$[\text{Starvation mortality}] = \begin{cases} 1, & \text{if } \frac{1}{1 + e^{k(\text{starving steps} - \beta\text{starvation})}} \\ 0, & \text{otherwise} \end{cases}$	Mortalities

Eq. 12	$[\text{Age mortality}] = \begin{cases} 1, & \text{if } [\beta\text{min} + (\beta\text{max} - \beta\_\text{min})e^{\frac{-\text{age}}{\beta\text{decay}}} \\ 0, & \text{otherwise} \end{cases}$	Mortalities
Eq. 13	$[\text{Constant mortality}] = \begin{cases} 1, & \text{if } \beta\text{constant} > U \\ 0, & \text{otherwise} \end{cases}$	Mortalities

681 Table 2. List of parameters used in the model.

Abbreviation	Description (units)	Values
Life cycle parameters		
βhunger	Hunger (KJ)	1000
βbasal	Basal energy expenditure (KJ)	βhunger/3.5
βloss	Energy loss from movement (KJ)	βbasal /8
βradius	Radius of movement (cells)	5
βdire, kdire	Parameters of movement directionality	βdire = -0.2, kdire = 30°
βholling	Constant in functional consumption	βhunger*0.9
βreproduction	Energy of reproduction (satiated steps)	450 (~52% non-breeding season)
βsupply	Energy cost of chick production and supply (KJ)	βhunger*0.1
βfledge	Number of provisioning events	110 (~once a day)
βstarvation	Starvation mortality (days without food)	10
βconstant	Annual constant mortality	1%
βmemory	Number of cells birds remember	30
Life history parameters		
βclutch	Clutch size (number of offspring)	Slow = 1, intermediate = 2, fast = 3
βfirstbreed	Age of first reproduction (years)	Slow = 9, intermediate = 4, fast = 3
βmin, βmax	Age-mortality (min-max exponential function)	Slow = 5-25%, intermediate = 15-35%, fast = 20-40%
βsenescence	Max age (years)	Slow = 40, intermediate = 25, fast = 20
Environmental parameters		
βmu, βsigma, βnu	Parameters of the energy raster (ZINBI)	βmu = 2, βsigma = 0.5, βnu = 0.2
βfood	Food multiplicator	3500
βreplenishment	Energy replenishment time (steps)	12

Trap parameters		
βproportion	Proportion of trapped area	5%, 15%, 25%
βwhere	Energy percentile threshold used to place traps. Traps occur in cells with energy ≥ specified percentile	0.9 (high-quality), 0 (random)
βsubsidy	Subsidized energy per cell (KJ)	Low = 500, medium = 1500, high = 3500
βlethality	Probability of mortality in trap-cells	Low = 2.50E-04, medium = 5.00E-04, high = 7.50E-04

682

683

684

685

686

687

688

689

690

691

692

693

694

695

696

697

Figures

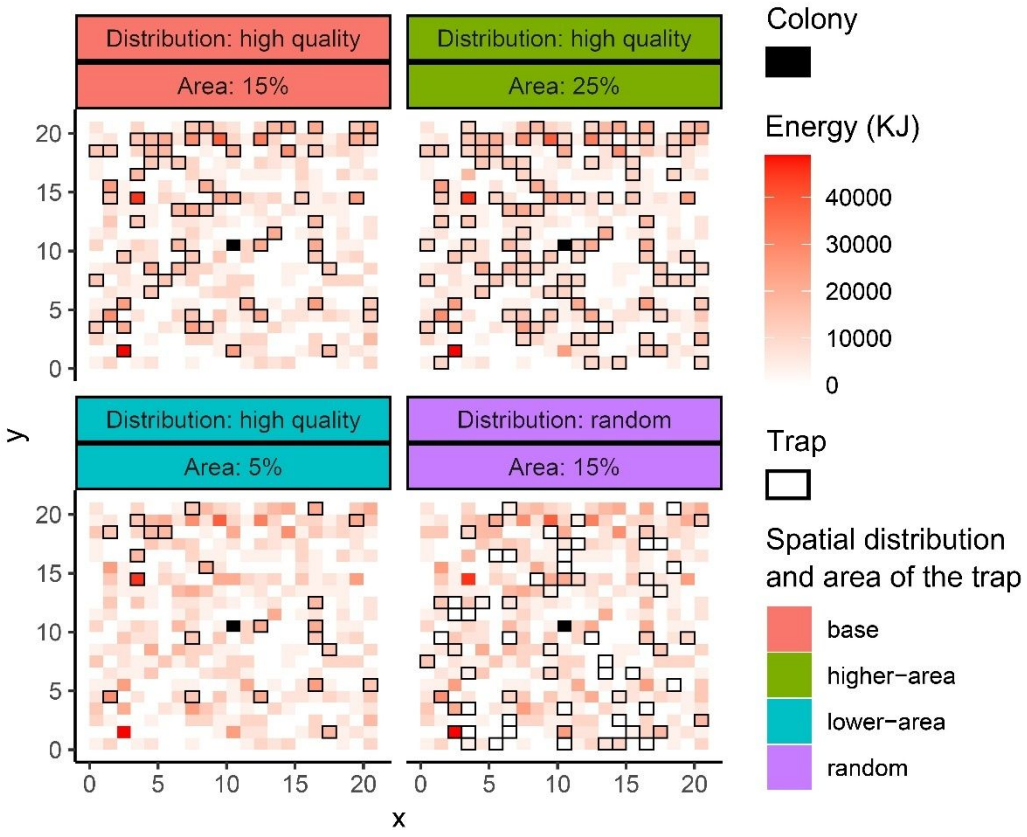

Figure 1. Model entities and spatial configuration of traps, showing variation in trap distribution (traps placed in high-quality habitat vs. randomly distributed traps) and trap area (5%, 15%, 25%). Each configuration was combined with three levels of bycatch mortality and three levels of trophic subsidies, resulting in 36 trap scenarios. Each scenario was simulated for the three life-history strategies and replicated seven times (see Figure 3). The energy raster represents the environment as a 21 × 21 grid, with energy values generated using a zero-inflated negative binomial distribution. The environment has a toroidal (donut-shaped) topology, allowing individuals to move seamlessly across edges. The colony is located at the center of the grid (x = 10, y = 10). The trap raster indicates the presence (black outline) or absence of a trap in each cell.

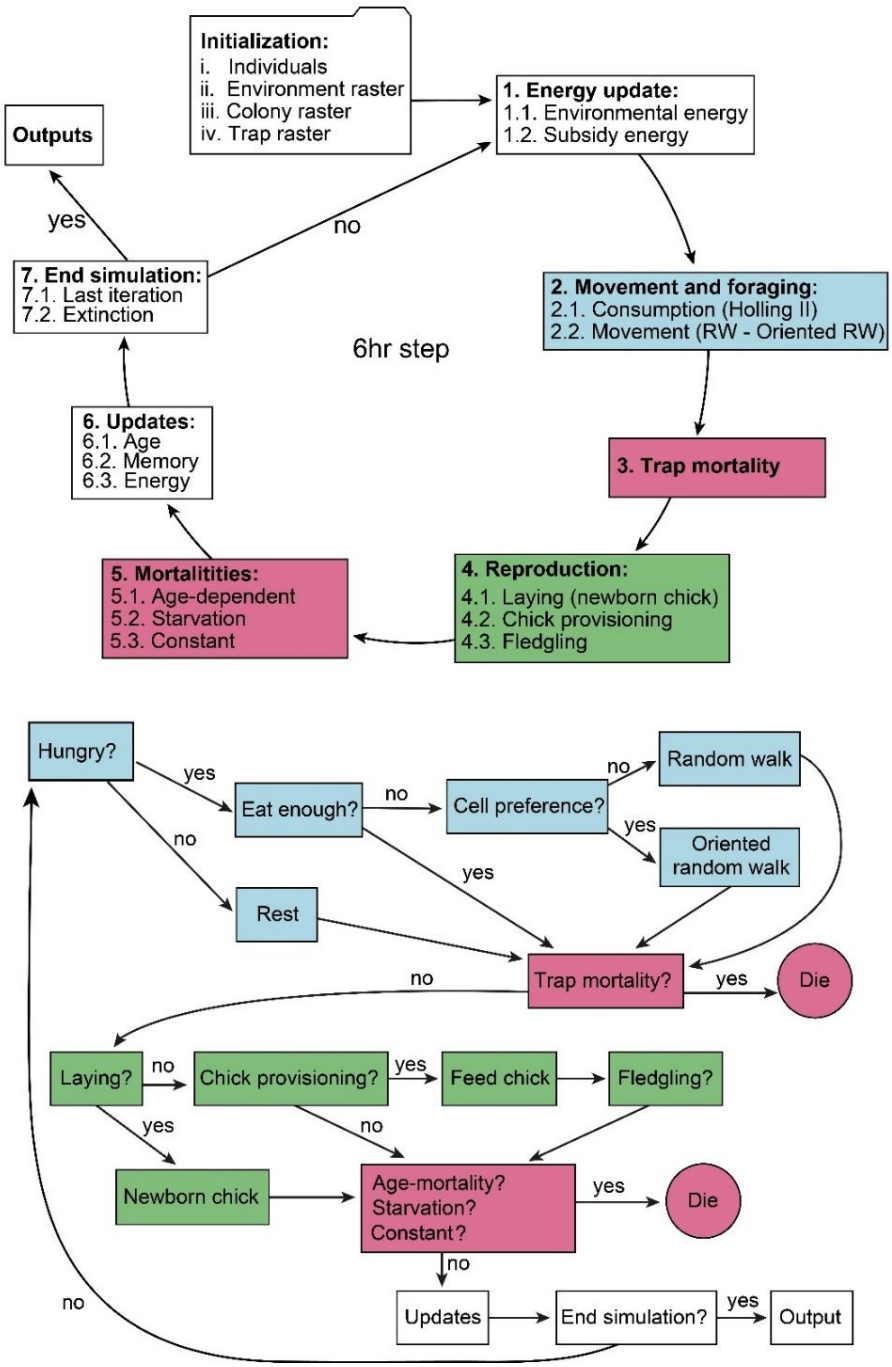

709

710 Figure 2. Overview of the program structure (top) and model components (bottom). The top panel
711 illustrates the sequence of all modules within the program, while the bottom panel provides a detailed

712 view of the algorithms governing the Movement and Foraging, Reproduction, and Mortality sub-
713 models, depicting the decision-making processes and actions performed by individuals throughout their
714 life cycle. The Reproduction sub-model (in green) is executed only during the reproductive season.

715

716

717

718

719

720

721

722

723

724

725

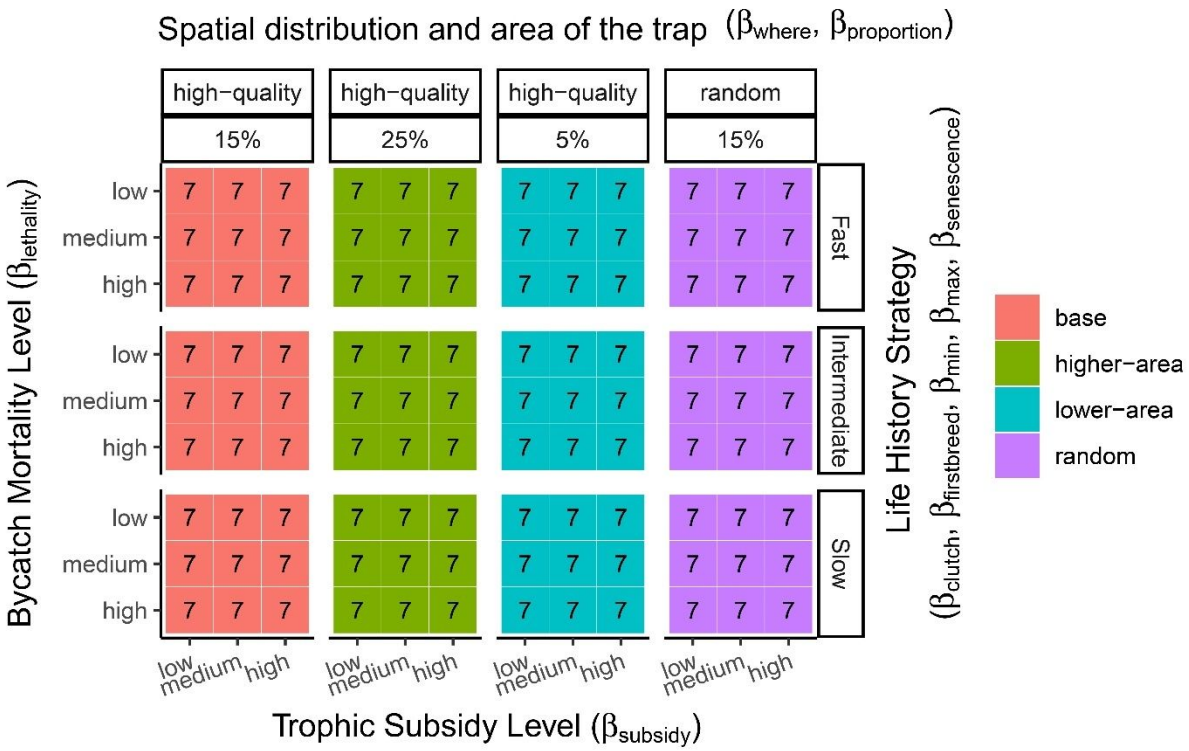

Figure 3. Diagram of all simulations evaluated across trap configurations. For each combination of trap distribution (high-quality vs. random) and trap area (5%, 15%, 25%), simulations were conducted under all combinations of bycatch mortality (3 levels), trophic subsidy (3 levels), and species' life-history strategies (3 types), resulting in a 3 × 3 × 3 matrix. The parameters (denoted with "β") associated with each variable are shown in parentheses (see Table 2). Each tile in the diagram represents a specific combination of these factors, with the number indicating the number of replicates (7). This design yielded a total of 756 simulations.

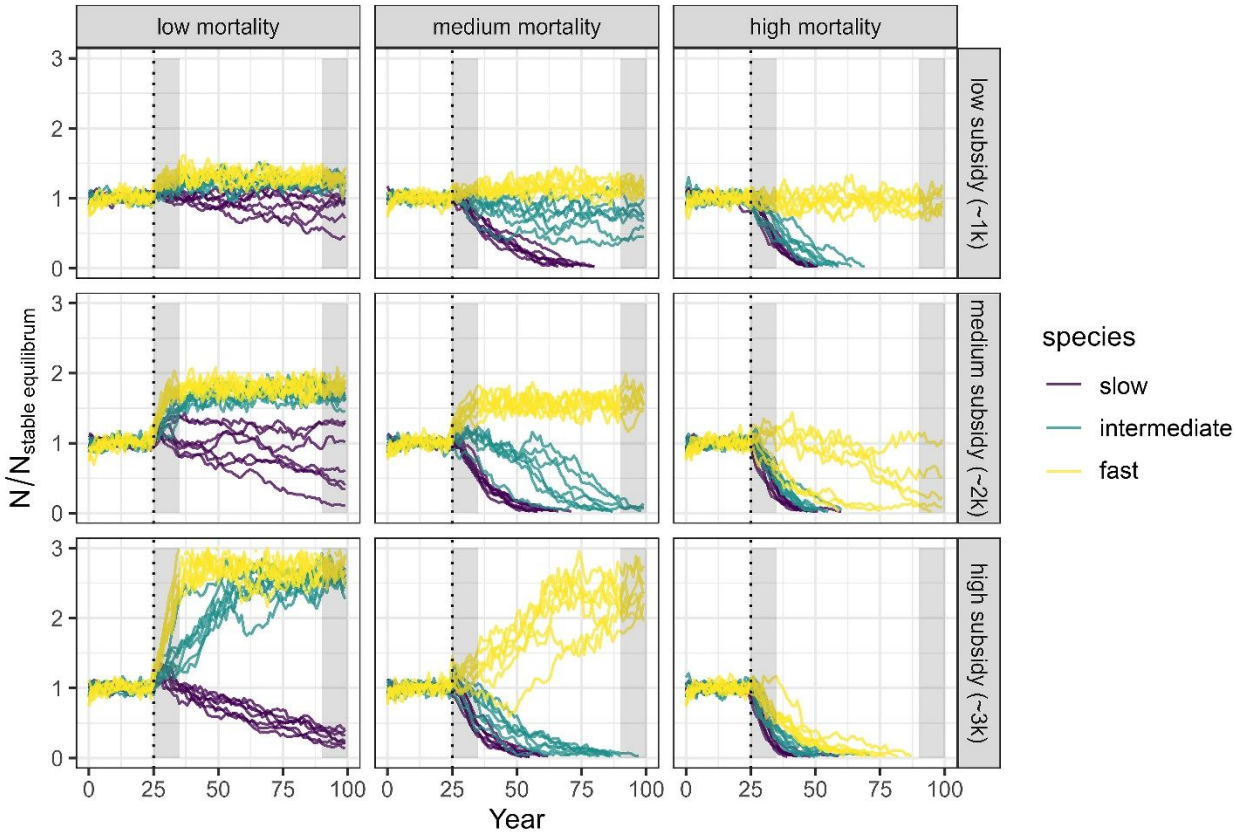

739

740 Figure 4. Population responses of species with different life histories—slow (albatross), intermediate
741 (gull), and fast (cormorant)—to a compensatory ecological trap involving a demographic trade-off
742 between decreased survival and increased recruitment due to trophic subsidies (n = 189 models; 3 life
743 histories × 3 subsidy levels × 3 mortality levels × 7 replicates). Population sizes are standardized to the
744 steady-state size observed in the first 24 years under control conditions. The ecological trap (base trap
745 configuration) is introduced continuously from year 25 onward (indicated by the dashed line). Gray bars
746 highlight short- and long-term responses (see Figure 5).

747

748

749

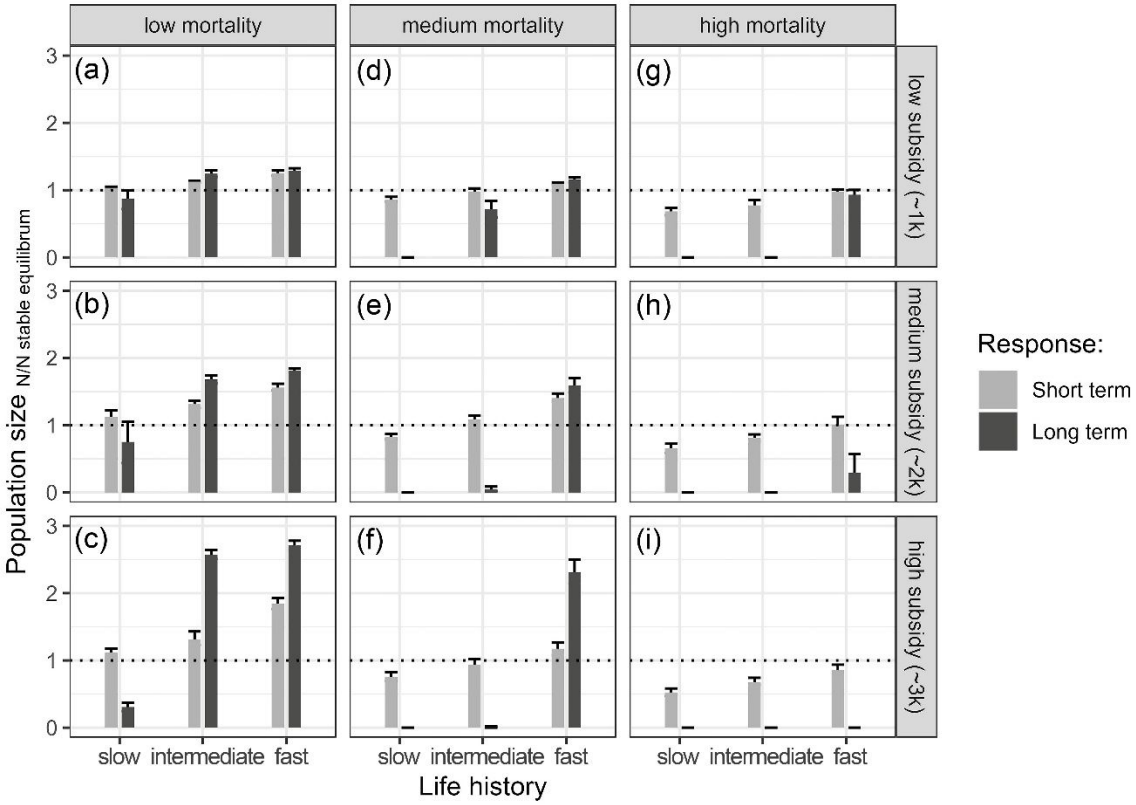

Figure 5. Short- and long-term population responses (mean ± bootstrapped 95% confidence interval) of species with varying life histories—slow (albatross), intermediate (gull), and fast (cormorant)—to a compensatory ecological trap involving a demographic trade-off between decreased survival and increased recruitment due to trophic subsidies (base trap configuration, n = 189 models; 3 life histories × 3 subsidy levels × 3 mortality levels × 7 replicates). Population sizes are standardized to the steady-state size observed in the first 24 years under control conditions.

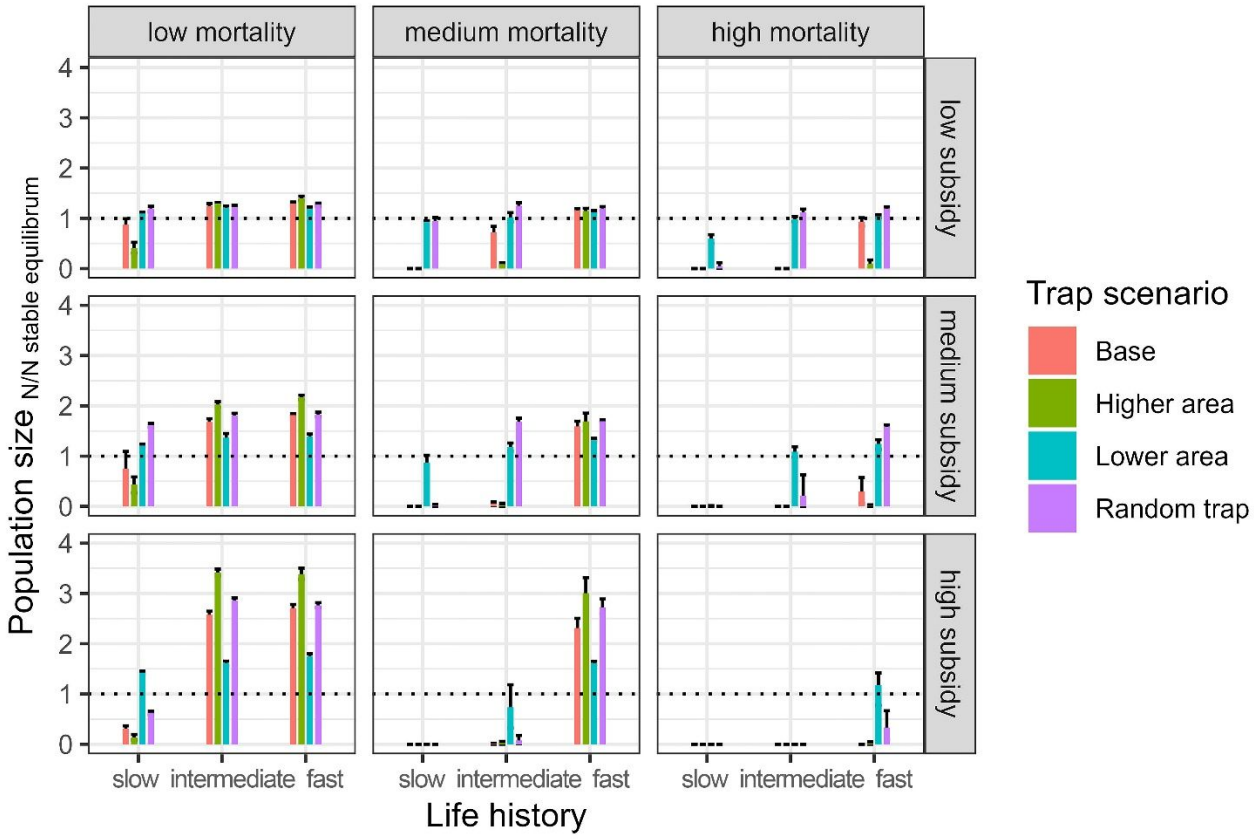

760

761 Figure 6. Long-term population responses (mean ± bootstrapped 95% confidence interval) of species
762 with varying life histories—slow (albatross), intermediate (gull), and fast (cormorant)—to the base trap
763 configuration, a larger-area trap (25% of the habitat), a smaller-area trap (5% of the habitat), and a
764 randomly distributed trap covering 15% of the habitat. Population sizes are standardized to the steady-
765 state size observed during the first 24 years under control conditions.

766

767

768

769

770

771

References

ACAP, 2024. ACAP Review of Mitigation Measures and Best Practice Advice for Reducing the Impact of Pelagic and Demersal Trawl Fisheries on Seabirds. Lima, Peru.

Anderson, O.R.J.J., Small, C.J., Croxall, J.P., Dunn, E.K., Sullivan, B.J., Yates, O., Black, A., 2011. Global seabird bycatch in longline fisheries. Endanger Species Res 14, 91–106. https://doi.org/10.3354/esr00347

Barbraud, C., Marteau, C., Ridoux, V., Delord, K., Weimerskirch, H., 2008. Demographic response of a population of white-chinned petrels Procellaria aequinoctialis to climate and longline fishery bycatch. Journal of Applied Ecology 45, 1460–1467. https://doi.org/10.1111/j.1365-2664.2008.01537.x

Barrett, T., Dowle, M., Srinivasan, A., Gorecki, J., Chirico, M., Hocking, T., Schwendinger, B., 2024. data.table: Extension of `data.frame`.

Battin, J., 2004. When Good Animals Love Bad Habitats: Ecological Traps and the Conservation of Animal populations. Conservation Biology 18, 1482–1491.

Bauduin, S., McIntire, E.J.B., Chubaty, A.M., 2019. NetLogoR: a package to build and run spatially explicit agent-based models in R. Ecography 42, 1841–1849. https://doi.org/10.1111/ecog.04516

Becker, D.J., Streicker, D.G., Altizer, S., 2015. Linking anthropogenic resources to wildlife-pathogen dynamics: A review and meta-analysis. Ecol Lett 18, 483–495. https://doi.org/10.1111/ele.12428

Bicknell, A.W.J., Oro, D., Camphuysen, K.C.J., Votier, S.C., 2013. Potential consequences of discard reform for seabird communities. Journal of Applied Ecology 50, 649–658. https://doi.org/10.1111/1365-2664.12072

Brown, J.H., 2004. Toward a metabolic theory of ecology. Ecology 85, 1771–1789.

Capdevila, P., Beger, M., Blomberg, S.P., Hereu, B., Linares, C., Salguero-Gómez, R., 2020. Longevity, body dimension and reproductive mode drive differences in aquatic versus terrestrial life-history strategies. Funct Ecol 34, 1613–1625. https://doi.org/10.1111/1365-2435.13604

Capdevila, P., Stott, I., Cant, J., Beger, M., Rowlands, G., Grace, M., Salguero-Gómez, R., 2022. Life history mediates the trade-offs among different components of demographic resilience. Ecol Lett 25, 1566–1579. https://doi.org/10.1111/ele.14004

Carmona, C.P., Tamme, R., Pärtel, M., De Bello, F., Brosse, S., Capdevila, P., González-M, R., González-Suárez, M., Salguero-Gómez, R., Vásquez-Valderrama, M., Toussaint, A., 2021. Erosion of global functional diversity across the tree of life. Sci. Adv 7.

Carneiro, A.P.B., Dias, M.P., Clark, B.L., Pearmain, E.J., Handley, J., Hodgson, A.R., Croxall, J.P., Phillips, R.A., Oppel, S., Morten, J.M., Lascelles, B., Cunningham, C., Taylor, F.E., Miller, M.G.R., Taylor, P.R., Bernard, A., Grémillet, D., Davies, T.E., 2024. The BirdLife Seabird Tracking Database: 20 years of collaboration for marine conservation. Biol Conserv 299. https://doi.org/10.1016/j.biocon.2024.110813

Charnov, E., 1976. Optimal foraging: The marginal value theorem. Theor Popul Biol 9, 129–136.

Clark, T.J., Luis, A.D., 2020. Nonlinear population dynamics are ubiquitous in animals. Nat Ecol Evol 4, 75–81. https://doi.org/10.1038/s41559-019-1052-6

Cleeland, J.B., Pardo, D., Raymond, B., Tuck, G.N., McMahon, C.R., Phillips, R.A., Alderman, R., Lea, M.A., Hindell, M.A., 2021. Disentangling the Influence of Three Major Threats on the Demography of an Albatross Community. Front Mar Sci 8. https://doi.org/10.3389/fmars.2021.578144

Cooke, R.S.C., Eigenbrod, F., Bates, A.E., 2019. Projected losses of global mammal and bird ecological strategies. Nat Commun 10. https://doi.org/10.1038/s41467-019-10284-z

Cooney, C.R., Sheard, C., Clark, A.D., Healy, S.D., Liker, A., Street, S.E., Troisi, C.A., Thomas, G.H., Székely, T., Hemmings, N., Wright, A.E., 2020. Ecology and allometry predict the evolution of avian developmental durations. Nat Commun 11. https://doi.org/10.1038/s41467-020-16257-x

Delibes, M., Gaona, P., Ferreras, P., 2001. Effects of an Attractive Sink Leading into Maladaptive Habitat Selection. Am Nat 158, 1–44.

Dias, M.P., Martin, R., Pearmain, E.J., Burfield, I.J., Small, C., Phillips, R.A., Yates, O., Lascelles, B., Borboroglu, P.G., Croxall, J.P., 2019. Threats to seabirds: A global assessment. Biol Conserv 237, 525–537. https://doi.org/10.1016/j.biocon.2019.06.033

Donovan, T.M., Thompson, F.R., 2001. Modeling The Ecological Trap Hypothesis: A Habitat and Demographic Analysis for Migrant Songbirds. Ecological Applications 11, 871–882. https://doi.org/10.2307/3061122

Dunn, R.E., White, C.R., Green, J.A., 2018. A model to estimate seabird field metabolic rates. Biol Lett 14. https://doi.org/10.1098/rsbl.2018.0190

Dwernychuk, L.W., Boag, D.A., 1972. Ducks nesting in association with gulls-an ecological trap? Can J Zool 50, 559–563.

Favero, M., Blanco, G., García, G., Copello, S., Seco Pon, J.P., Frere, E., Quintana, F., Yorio, P., Rabuffetti, F., Cañete, G., 2011. Seabird mortality associated with ice trawlers in the Patagonian shelf: effect of discards on the occurrence of interactions with fishing gear. Anim Conserv 14, 131–139. https://doi.org/10.1111/j.1469-1795.2010.00405.x

Fletcher, R.J., Orrock, J.L., Robertson, B.A., 2012. How the type of anthropogenic change alters the consequences of ecological traps. Proceedings of the Royal Society B 279, 2546–2552. https://doi.org/10.1098/rspb.2011.0139

Gaillard, J.M., Lemaître, J.F., Berger, V., Bonenfant, C., Devillard, S., Douhard, M., Gamelon, M., Plard, F., Lebreton, J.D., 2016. Life Histories, Axes of Variation, in: Kliman, R.M. (Ed.), Encyclopedia of Evolutionary Biology. Oxford: Academic Press, pp. 312–323. https://doi.org/10.1016/B978-0-12-800049-6.00085-8

Garthe, S., Camphuysen, K., Furness, R.W., 1996. Amounts of discards by commercial fisheries and their significance as food for seabirds in the North Sea. Mar Ecol Prog Ser 136, 1–11. https://doi.org/10.3354/meps136001

Gates, J.E., Gysel, L.W., 1978. Avian nest dispersion and fledging success in field-forest ecotones. Ecology 59, 871–883.

Genovart, M., Arcos, J.M., Alvarez, D., McMinn, M., Meier, R., Wynn, R.B., Guilford, T., Oro, D., Álvarez, D., McMinn, M., Meier, R., B. Wynn, R., Guilford, T., Oro, D., 2016. Demography of the critically endangered Balearic shearwater: the impact of fisheries and time to extinction. Journal of Applied Ecology 53, 1158–1168. https://doi.org/10.1111/1365-2664.12622

Genovart, M., Doak, D.F., Igual, J.M., Sponza, S., Kralj, J., Oro, D., 2017. Varying demographic impacts of different fisheries on three Mediterranean seabird species. Glob Chang Biol 23, 3012–3029. https://doi.org/10.1111/gcb.13670

Gilman, E., Perez Roda, A., Huntington, T., Kennelly, S.J., Suuronen, P., Chaloupka, M., Medley, P.A.H., 2020. Benchmarking global fisheries discards. Sci Rep 10. https://doi.org/10.1038/s41598-020-71021-x

González-Zevallos, D., Yorio, P., 2006. Seabird use of discards and incidental captures at the Argentine hake trawl fishery in the Golfo San Jorge, Argentina. Mar Ecol Prog Ser 316, 175–183. https://doi.org/10.3354/meps316175

Grémillet, D., Pichegru, L., Kuntz, G., Woakes, A.G., Wilkinson, S., Crawford, R.J.M., Ryan, P.G., 2008. A junk-food hypothesis for gannets feeding on fishery waste. Proceedings of the Royal Society B: Biological Sciences 275, 1149–1156. https://doi.org/10.1098/rspb.2007.1763

Grimm, V., Berger, U., Bastiansen, F., Eliassen, S., Ginot, V., Giske, J., Goss-Custard, J., Grand, T., Heinz, S.K., Huse, G., Huth, A., Jepsen, J.U., Jørgensen, C., Mooij, W.M., Müller, B., Pe'er, G., Piou, C., Railsback, S.F., Robbins, A.M., Robbins, M.M., Rossmanith, E., Rüger, N., Strand, E., Souissi, S., Stillman, R.A., Vabø, R., Visser, U., DeAngelis, D.L., 2006. A standard protocol for describing individual-based and agent-based models. Ecol Modell 198, 115–126. https://doi.org/10.1016/j.ecolmodel.2006.04.023

Grimm, V., Railsback, S.F., 2005. Individual-based modeling and ecology. Princeton university press, princeton, New Jersey.

Hale, R., Swearer, S.E., 2016. Ecological traps: Current evidence and future directions. Proceedings of the Royal Society B 283. https://doi.org/10.1098/rspb.2015.2647

Hale, R., Treml, E.A., Swearer, S.E., 2015. Evaluating the metapopulation consequences of ecological traps. Proceedings of the Royal Society B: Biological Sciences 282. https://doi.org/10.1098/rspb.2014.2930

Hatton, I.A., Dobson, A.P., Storch, D., Galbraith, E.D., Loreau, M., 2019. Linking scaling laws across eukaryotes. Proc Natl Acad Sci U S A 116, 21616–21622. https://doi.org/10.1073/pnas.1900492116

Heppell, S.S., Caswell, H., Crowder, L.B., 2000. Life histories and elasticity patterns: Perturbation analysis for species with minimal demographic data. Ecology 81, 654–665. https://doi.org/10.1890/0012-9658(2000)081[0654:LHAEPP]2.0.CO;2

Herrando-Pérez, S., Delean, S., Brook, B.W., Bradshaw, C.J.A., 2012. Strength of density feedback in census data increases from slow to fast life histories. Ecol Evol 2, 1922–1934. https://doi.org/10.1002/ece3.298

Holling, C.S., 1959. Some characteristics of simple types of predation and parasitism. Can Entomol 91, 385–398.

Karpouzi, V.S., Watson, R., Pauly, D., 2007. Modelling and mapping resource overlap between seabirds and fisheries on a global scale: A preliminary assessment. Mar Ecol Prog Ser 343, 87–99. https://doi.org/10.3354/meps06860

Kokko, H., Sutherland, W.J., 2001. Ecological traps in changing environments: Ecological and evolutionary consequences of a behaviourally mediated Allee effect. Evol Ecol Res 3, 537–551.

Kristan, William B, Kristan, I., Kristan, W B, 2003. The role of habitat selection behavior in population dynamics: source-sink systems and ecological traps. Oikos 103, 457–468.

Lamb, C.T., Mowat, G., McLellan, B.N., Nielsen, S.E., Boutin, S., 2017. Forbidden fruit: human settlement and abundant fruit create an ecological trap for an apex omnivore. Journal of Animal Ecology 86, 55–65. https://doi.org/10.1111/1365-2656.12589

Langlois Lopez, S., Bond, A.L., O'Hanlon, N.J., Wilson, J.M., Vitz, A., Mostello, C.S., Hamilton, F., Rail, J.F., Welch, L., Boettcher, R., Wilhelm, S.I., Anker-Nilssen, T., Daunt, F., Masden, E., 2023. Global population and conservation status of the Great Black-backed Gull Larus marinus. Bird Conserv Int 33. https://doi.org/10.1017/S0959270922000181

Lewison, R.L., Crowder, L.B., Wallace, B.P., Moore, J.E., Cox, T., Zydelis, R., McDonald, S., DiMatteo, A., Dunn, D.C., Kot, C.Y., Bjorkland, R., Kelez, S., Soykan, C., Stewart, K.R., Sims, M., Boustany, A., Read, A.J., Halpin, P., Nichols, W.J., Safina, C., 2014. Global patterns of marine mammal, seabird, and sea turtle bycatch reveal taxa-specific and cumulative megafauna hotspots. Proceedings of the National Academy of Sciences 111, 5271–5276. https://doi.org/10.1073/pnas.1318960111

Morris, D.W., 2005. Paradoxical avoidance of enriched habitats: Have we failed to appreciate omnivores? Ecology 86, 2568–2577. https://doi.org/10.1890/04-0909

Munstermann, M.J., Heim, N.A., McCauley, D.J., Payne, J.L., Upham, N.S., Wang, S.C., Knope, M.L., 2022. A global ecological signal of extinction risk in terrestrial vertebrates. Conservation Biology 36. https://doi.org/10.1111/cobi.13852

Oro, D., 1996. Effects of trawler discard availability on egg laying and breeding success in the lesser black-backed gull Larus fuscus in the western Mediterranean. Mar Ecol Prog Ser 132, 43–46.

Oro, D., Bosch, M., Ruiz, X., 1995. Effects of a trawling moratorium on the breeding success of the Yellow-legged Gull Larus cachinnans. International Journal of Avian Science 137, 547–549.

Oro, D., Genovart, M., Tavecchia, G., Fowler, M.S., Martínez-Abraín, A., 2013. Ecological and evolutionary implications of food subsidies from humans. Ecol Lett 16, 1501–1514. https://doi.org/10.1111/ele.12187

Oro, D., Jover, L., Ruiz, X., 1996. Influence of trawling activity on the breeding ecology of a threatened seabird, Audouin\'s gull Larus audouinii. Mar Ecol Prog Ser 139, 19–29.

Pardo, D., Forcada, J., Wood, A.G., Tuck, G.N., Ireland, L., Pradel, R., Croxall, J.P., Phillips, R.A., 2017. Additive effects of climate and fisheries drive ongoing declines in multiple albatross species. Proceedings of the National Academy of Sciences 114, E10829–E10837. https://doi.org/10.1073/pnas.1618819114

Peters, R.H., 1983. The Ecological Implications of Body Size, The Ecological Implications of Body Size. Cambridge University Press. https://doi.org/10.1017/cbo9780511608551

Phillips, R.A., Fox, E., Crawford, R., Prince, S., Yates, O., 2024. Incidental mortality of seabirds in trawl fisheries: A global review. Biol Conserv 296. https://doi.org/10.1016/j.biocon.2024.110720

Pikitch, E.K., Santora, C., Babcock, E.A., Bakun, A., Bonfil, R., Conover, D.O., Dayton, P., Doukakis, P., Fluharty, D., Heneman, B., 2004. Ecosystem-based fishery management. Science (1979) 305, 346–347.

R Core Team, 2021. R: A language and environment for statistical computing.

Railsback, S.F., 2022. Suboptimal foraging theory: How inaccurate predictions and approximations can make better models of adaptive behavior. Ecology 103. https://doi.org/10.1002/ecy.3721

Richards, C., Cooke, R., Bowler, D.E., Boerder, K., Bates, A.E., 2024. Bycatch-threatened seabirds disproportionally contribute to community trait composition across the world. Glob Ecol Conserv 49. https://doi.org/10.1016/j.gecco.2023.e02792

Richards, C., Cooke, R.S.C.C., Bates, A.E., 2021. Biological traits of seabirds predict extinction risk and vulnerability to anthropogenic threats. Global Ecology and Biogeography 30, 973–986. https://doi.org/10.1111/geb.13279

Rigby, R.A., Stasinopoulos, M.D., Heller, G.Z., De Bastiani, F., 2019. Distributions for modeling location, scale, and shape: Using GAMLSS in R. Chapman and Hall/CRC.

Robert Burger, J., Hou, C., A. S. Hall, C., Brown, J.H., 2021. Universal rules of life: metabolic rates, biological times and the equal fitness paradigm. Ecol Lett. https://doi.org/10.1111/ele.13715

Robertson, B.A., Blumstein, D.T., 2019. How to disarm an evolutionary trap. Conserv Sci Pract e116. https://doi.org/10.1111/csp2.116

Robertson, B.A., Rehage, J.S., Sih, A., 2013. Ecological novelty and the emergence of evolutionary traps. Trends Ecol Evol 28, 552–560. https://doi.org/10.1016/j.tree.2013.04.004

Rodewald, A.D., Kearns, L.J., Shustack, D.P., 2011. Anthropogenic resource subsidies decouple predator-prey relationships. Ecological Applications 21, 936–943.

Rogers, T.L., Johnson, B.J., Munch, S.B., 2022. Chaos is not rare in natural ecosystems. Nat Ecol Evol 6, 1105–1111.

Rolland, V., Barbraud, C., Weimerskirch, H., 2009. Assessing the impact of fisheries, climate and disease on the dynamics of the Indian yellow-nosed Albatross. Biol Conserv 142, 1084–1095. https://doi.org/10.1016/j.biocon.2008.12.030

Rolland, V., Barbraud, C., Weimerskirch, H., 2008. Combined effects of fisheries and climate on a migratory long-lived marine predator. Journal of Applied Ecology 45, 4–13. https://doi.org/10.1111/j.1365-2664.2007.01360.x

Rolland, V., Weimerskirch, H., Barbraud, C., 2010. Relative influence of fisheries and climate on the demography of four albatross species. Glob Chang Biol 16, 1910–1922. https://doi.org/10.1111/j.1365-2486.2009.02070.x

Saether, B.-E., 1987. The influence of body weight on the covariation between reproductive traits in European birds. Oikos 48, 79–88.

Saether, B.-E., Bakke, Ø., 2000. Avian life history variation and contribution of demographic traits to the population growth rate. Ecology 81, 642–653.

Sæther, B.E., Engen, S., Møller, A.P., Weimerskirch, H., Visser, M.E., Fiedler, W., Matthysen, E., Lambrechts, M.M., Badyaev, A., Becker, P.H., Brommer, J.E., Bukacinski, D., Bukacinska, M., Christensen, H., Dickinson, J., Du Feu, C., Gehlbach, F.R., Heg, D., Hötker, H., Merilä, J., Nielsen, J.T., Rendell, W., Robertson, R.J., Thomson, D.L., Török, J., Van Hecke, P., 2004. Life-history variation predicts the effects of demographic stochasticity on avian population dynamics. American Naturalist 164, 793–802. https://doi.org/10.1086/425371

Sánchez-Clavijo, L.M., Hearns, J., Quintana-Ascencio, P.F., 2016. Modeling the effect of habitat selection mechanisms on population responses to landscape structure. Ecol Modell 328, 99–107. https://doi.org/10.1016/j.ecolmodel.2016.03.004

Scales, K.L., Hazen, E.L., Jacox, M.G., Castruccio, F., Maxwell, S.M., Lewison, R.L., Bograd, S.J., 2018. Fisheries bycatch risk to marine megafauna is intensified in Lagrangian coherent structures. Proc Natl Acad Sci U S A 115, 7362–7367. https://doi.org/10.1073/pnas.1801270115

Schreiber, E.A., Burger, J. (Eds.), 2001. Biology of marine birds, Book. CRS Press, Boca Raton, Florida. https://doi.org/10.1650/0010-5422(2003)105[0392:BR]2.0.CO;2

Semeniuk, C.A.D., Rothley, K.D., 2008. Costs of group-living for a normally solitary forager: Effects of provisioning tourism on southern stingrays Dasyatis americana. Mar Ecol Prog Ser 357, 271–282. https://doi.org/10.3354/meps07299

Sherley, R.B., Ladd-Jones, H., Garthe, S., Stevenson, O., Votier, S.C., 2019. Scavenger communities and fisheries waste: North Sea discards support 3 million seabirds, 2 million fewer than in 1990. Fish and Fisheries 21, 132–145. https://doi.org/10.1111/faf.12422

Sibly, R.M., Grimm, V., Martin, B.T., Johnston, A.S.A., Kulakowska, K., Topping, C.J., Calow, P., Nabe-Nielsen, J., Thorbek, P., Deangelis, D.L., 2013. Representing the acquisition and use of energy by individuals in agent-based models of animal populations. Methods Ecol Evol 4, 151–161. https://doi.org/10.1111/2041-210x.12002

Sibly, R.M., Witt, C.C., Wright, N.A., Venditti, C., Jetz, W., Brown, J.H., 2012. Energetics, lifestyle, and reproduction in birds. Proc Natl Acad Sci U S A 109, 10937–10941. https://doi.org/10.1073/pnas.1206512109

Sigaud, M., Merkle, J.A., Cherry, S.G., Fryxell, J.M., Berdahl, A., Fortin, D., 2017. Collective decision-making promotes fitness loss in a fusion-fission society. Ecol Lett 20, 33–40. https://doi.org/10.1111/ele.12698

Simeone, A., Anguita, C., M, D., Arce, P., Vega, R., Luna-Jorquera, G., Portflitt-Toro, M., Suazo, C., Miranda-Urbina, D., Ulloa, M., 2020. Spatial and temporal patterns of beached seabirds along the Chilean coast: Linking mortalities with commercial fisheries. Biol Conserv 256.

Simon, R.N., Fortin, D., 2020. Crop raiders in an ecological trap: optimal foraging individual-based modeling quantifies the effect of alternate crops. Ecological Applications 30. https://doi.org/10.1002/eap.2111

Stearns, S.C., 1992. The evolution of life histories. Oxford University Press, New York.

Sullivan, B.J., Reid, T.A., Bugoni, L., 2006. Seabird mortality on factory trawlers in the Falkland Islands and beyond. Biol Conserv 1, 495–504. https://doi.org/10.1016/j.biocon.2006.02.007

Swearer, S.E., Morris, R.L., Barrett, L.T., Sievers, M., Dempster, T., Hale, R., 2021. An overview of ecological traps in marine ecosystems. Front Ecol Environ 19, 234–242. https://doi.org/10.1002/fee.2322

Tuck, G.N., Thomson, R.B., Barbraud, C., Delord, K., Louzao, M., Herrera, M., Weimerskirch, H., 2015. An integrated assessment model of seabird population dynamics: can individual heterogeneity in susceptibility to fishing explain abundance trends in Crozet wandering albatross? Journal of Applied Ecology 52, 950–959. https://doi.org/10.1111/1365-2664.12462

Véran, S., Gimenez, O., Flint, E., Kendall, W.L., Doherty, P.F., Lebreton, J.D., Veran, S., Gimenez, O., Flint, E., Kendall, W.L., Doherty, P.F., Lebreton, J.D., 2007. Quantifying the impact of longline fisheries on adult survival in the black-footed albatross. Journal of Applied Ecology 44, 942–952. https://doi.org/10.1111/j.1365-2664.2007.01346.x

997 Votier, S.C., Furness, R.W., Bearhop, S., Crane, J.E., Caldow, R.W.G., Catry, P., Ensor, K., Hamer, K.C., Hudson, A.
998 V., Kalmbach, E., Klomp, N.I., Pfeiffer, S., Phillips, R.A., Prieto, I., Thompson, D.R., 2004. Changes in
999 fisheries discard rates and seabird communities. Nature 427, 727–730.
1000 https://doi.org/10.1038/nature02315

1001 Watkins, B.P., Petersen, S.L., Ryan, P.G., 2008. Interactions between seabirds and deep-water hake trawl gear :
1002 an assessment of impacts in South African waters. Animal consevation 11, 247–254.
1003 https://doi.org/10.1111/j.1469-1795.2008.00192.x

1004 Welch, H., Clavelle, T., White, T.D., Cimino, M.A., Kroodsma, D., Hazen, E.L., 2024. Unseen overlap between
1005 fishing vessels and top predators in the northeast Pacific. Sci Adv 10, 1.

1006 Wickham, H., François, R., Henry, L., Müller, K., Vaughan, D., 2023. dplyr: A Grammar of Data Manipulation.

1007 Wilhelm, S.I., Rail, J.F., Regular, P.M., Gjerdrum, C., Robertson, G.J., 2016. Large-Scale Changes in Abundance of
1008 Breeding Herring Gulls (Larus argentatus) and Great Black-Backed Gulls (Larus marinus) Relative to
1009 Reduced Fishing Activities in Southeastern Canada. Waterbirds 39, 136–142.
1010 https://doi.org/10.1675/063.039.sp104

1011 Žydelis, R., Small, C., French, G., 2013. The incidental catch of seabirds in gillnet fisheries: A global review. Biol
1012 Conserv 162, 76–88. https://doi.org/10.1016/j.biocon.2013.04.002

1013

1014

1015

1016

1017

1018

1019

1020

1021

1022

1023

1024

1025

Supplementary material

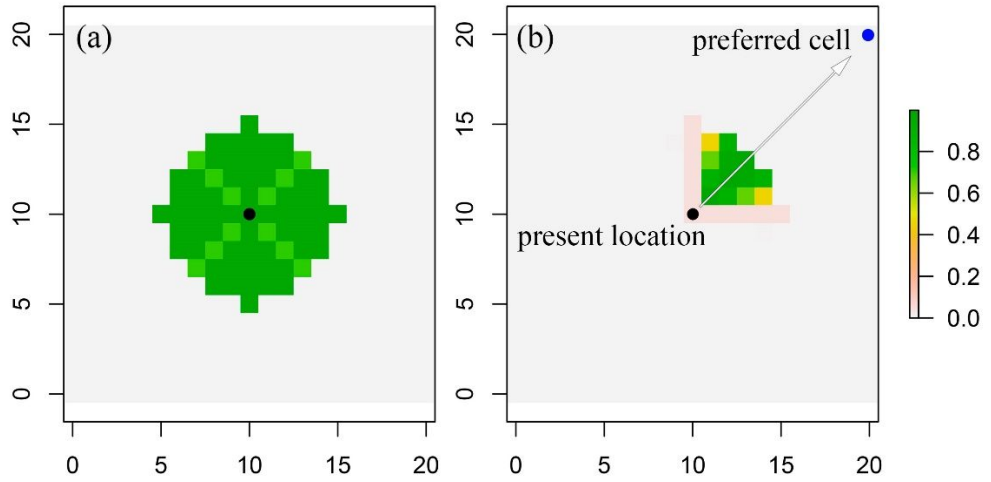

Figure S1. Diagram illustrating how movement probabilities are assigned to cells within the movement radius of an individual (located at the colony, x=10, y=10, in the example), both without (a) and with (b) cell preference. In (a) all cells within the movement radius are assigned equal probability (1), except for diagonal cells, which are penalized (0.7) to maintain isotropic movement. In (b), higher probabilities are assigned to cells in the direction of the preferred cell (blue cell at x = 20, y = 20, in the example). The figure illustrates the probabilities assigned using the chosen parameters (βkdire= −0.2 and βdire=30°, see Figure S2).

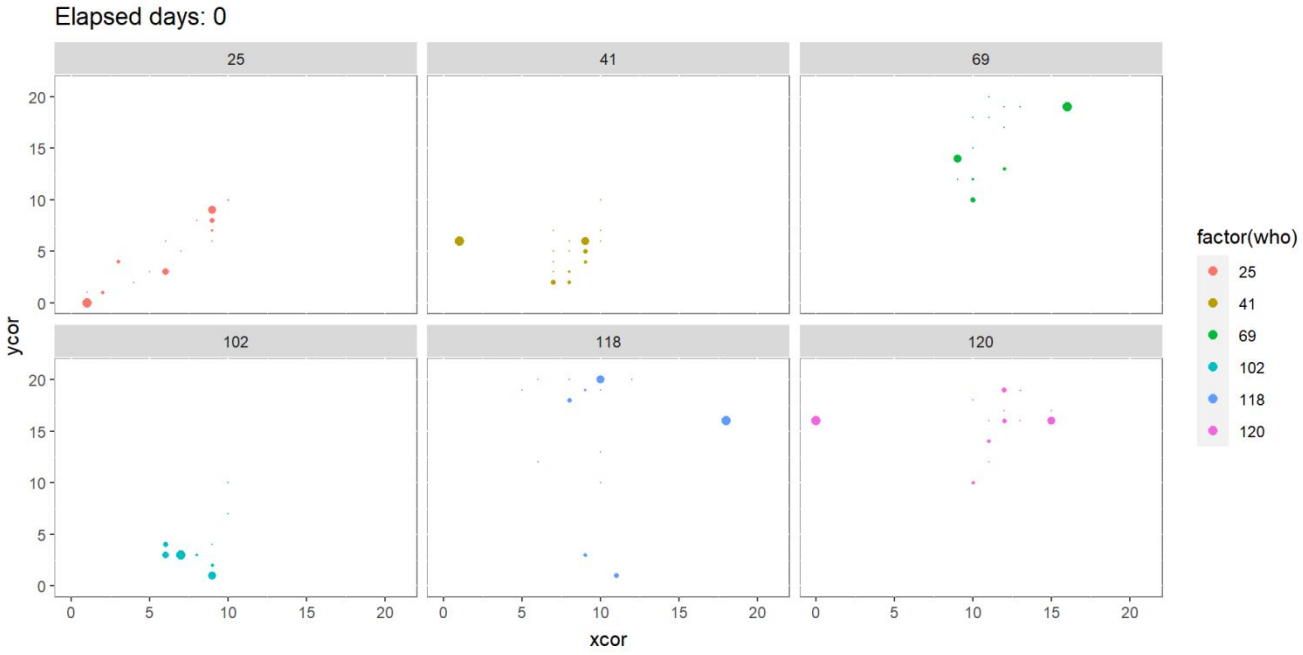

Figure S2. Animation illustrating the movement of individuals with habitat preference across cells. The annual cycle of six randomly selected individuals in the base model is displayed, with a fade effect applied to their locations to enhance visualization. On day 219, the reproductive season begins, and the individuals return to the colony at the center of the raster (x = 10, y = 10) to feed their chick.

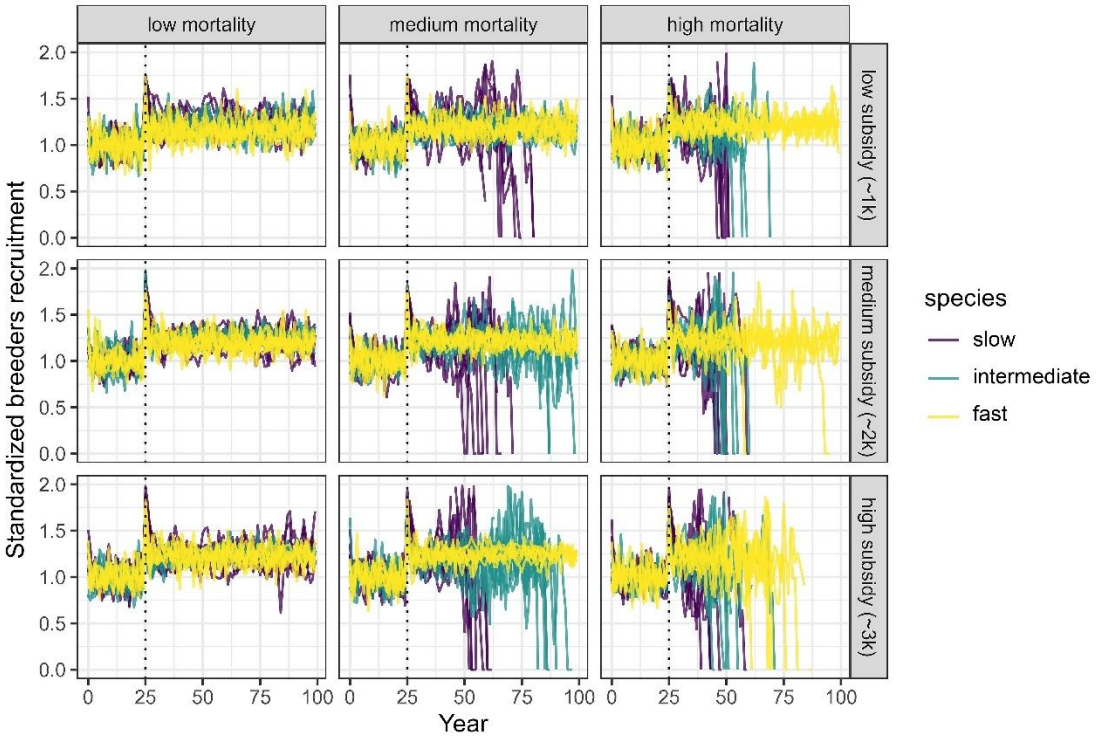

Figure S3. Breeders recruitment in species with varying life histories—slow (albatross), intermediate (gull), and fast (cormorant)—in the base trap configuration (n = 189 models; 3 life histories × 3 subsidy levels × 3 mortality levels × 7 replicates). The dashed line indicates the start of the trap. The proportion of breeders relative to the total number of potential breeders is shown, standardized to the average values observed during the first 24 years under control conditions.

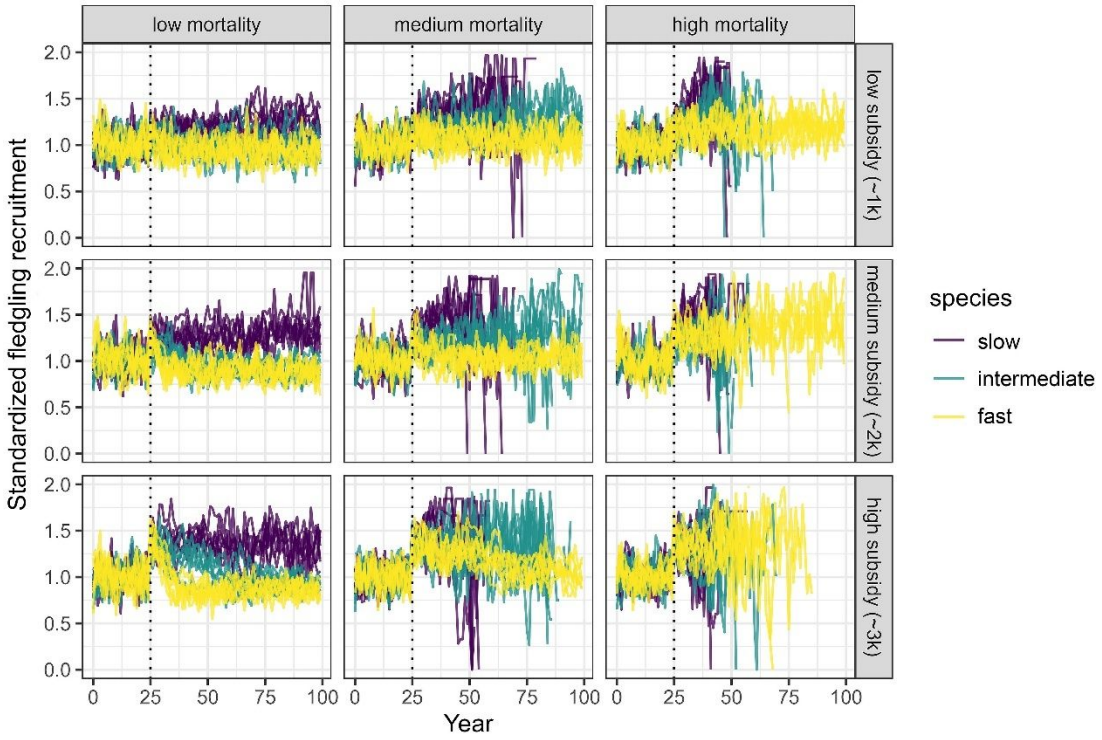

Figure S4. Fledgling recruitment in species with varying life histories—slow (albatross), intermediate (gull), and fast (cormorant)—in the base trap configuration (n = 189 models; 3 life histories × 3 subsidy levels × 3 mortality levels × 7 replicates). The dashed line indicates the start of the trap. Recruitment is expressed as the number of fledglings per breeder, standardized to the average values observed during the first 24 years under control conditions.

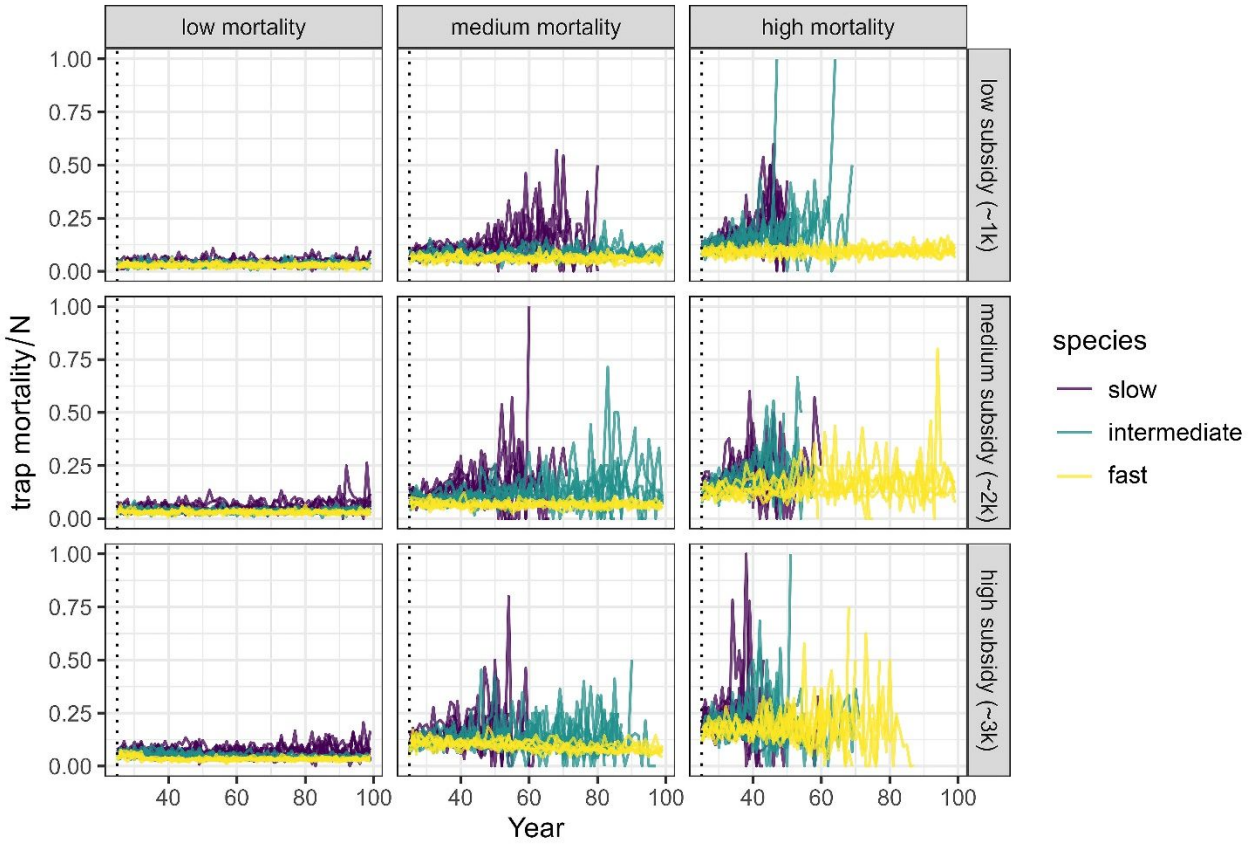

Figure S5. Effective trap mortality of species with varying life histories—slow (albatross), intermediate (gull), and fast (cormorant)—in the base trap configuration (n = 189 models; 3 life histories × 3 subsidy levels × 3 mortality levels × 7 replicates).